

Optimal Joint Decoding of Correlated Data Over Orthogonal Multiple Access Channels with Memory

Seyed Parsa Beheshti, Fady Alajaji, *Senior Member, IEEE*, and
Tamás Linder, *Fellow, IEEE*

Abstract

Motivated by the structure of basic sensor networks, we study an optimal joint decoding problem in which the real valued outputs of two correlated Gaussian sources are scalar quantized, bit assigned, and transmitted, without applying any channel coding or interleaving, over a multiple access channel (MAC) which consists of two orthogonal point-to-point time-correlated Rayleigh fading sub-channels used with soft-decision demodulation. Each fading sub-channel is modeled by a non-binary Markov noise discrete channel which was recently shown to effectively represent it. The correlated sources have memory captured by a time-varying correlation coefficient governed by a two-state first-order Markov process. At the receiver side, we design a joint sequence maximum a posteriori (MAP) decoder to exploit the correlation between the two sources, their temporal memory, as well as the redundancy left in the quantizers' indices, the channels' soft-decision outputs, and noise memory. Under the simple practical case of using two-level source quantization, we propose a Markov model to estimate the joint behavior of the quantized sources. We then establish necessary and a sufficient conditions under which the delay-prone joint sequence MAP decoder can be reduced to a simple instantaneous symbol-by-symbol decoder. We illustrate our analytical results by system simulation and demonstrate that joint MAP decoding can appropriately harness the source and channel characteristics to achieve improved signal-to-distortion ratio performance for a wide range of system conditions.

Index Terms: Sensor networks, joint source-channel MAP decoding, correlated Gaussian sources, Markov models, multiple access channels with memory, time-correlated fading, quantization.

S. P. Beheshti was with Queen's University, Kingston, ON, Canada; he is now with Bombardier Transportation. F. Alajaji and T. Linder are with the Department of Mathematics and Statistics and the Department of Electrical and Computer Engineering, Queen's University, Kingston, ON, Canada. This work was supported in part by NSERC of Canada. Parts of this work were presented at the IEEE Vehicular Technology Conference, Vancouver, Fall 2014 [1].

I. INTRODUCTION

In recent years, wireless sensor networks (WSN) have found many applications ranging from surveying physical or environmental conditions to industrial process monitoring and control [2]. In a WSN, spatially distributed autonomous sensors share and convey the observed data to a main base station which acts as a gateway between the sensor nodes and the end user. Given that sensors have very limited resources in energy, storage memory, computational speed, and communications bandwidth, it is not practical for them to form large queues of data or perform complex processing and source and channel coding operations. On the other hand, base stations have significantly more resources and can hence carry the brunt of the processing tasks needed to reliably recover the transmitted data captured by the sensors [3], [4].

In this work, we study a basic WSN modeled via a two-user multiple access channel (MAC) system where each sensor independently samples a real-valued parameter, such as humidity and temperature, and the samples in general exhibit temporal memory and are correlated to each other. The observed correlated data are governed by a bivariate Gaussian process whose correlation coefficient varies over time according to a two-state first-order Markov chain. We adopt a joint source-channel (JSC) coding approach, which has proven to be a considerably better alternative to traditional tandem separate source and channel coding under stringent complexity and delay constraints, e.g., see [5]–[15] and the references therein. These works illustrate the benefits of JSC coding from a theoretical (asymptotic analysis) perspective or investigate designs that employ source or channel codes (or a combination thereof), which may in practice demand substantial resources at the transmitter. In contrast, we focus in this work on a design which shifts the system's complexity and delay to the receiver side (which possesses more resources in a typical WSN) and makes the transmitter significantly simpler with zero transmission delay. More specifically, we investigate the optimal joint sequence maximum a posteriori (MAP) decoding problem when the correlated Gaussian sources are, at each node, scalar quantized and sent without the use of error-correcting codes and channel interleaving over an orthogonal MAC. The MAC is composed of two orthogonal sub-channels, where each sub-channel is a point-to-point time-correlated Rayleigh discrete fading channel (DFC) used with antipodal signaling

and soft-decision (non-binary) output quantization. However, as the Rayleigh DFC is hard to treat analytically [16], we instead use the recently introduced non-binary noise discrete channel with queue based noise (NBNDQ-QB) which has been shown to efficiently model such DFC [17]. The NBNDQ-QB aptly incorporates the benefits of channel memory and soft-decision information of the underlying DFC, yielding an analytically tractable model whose capacity can be measurably larger than the memoryless counterpart channel (realized via ideal infinite-depth block interleaving) or a channel with hard-decision outputs.¹

This problem belongs to the area of JSC decoding such as [16], [21]–[29], which study JSC decoding for various single-user systems (using a point-to-point channel). In particular, the problem we study here significantly generalizes the point-to-point MAP decoding problem examined in [16] as it involves the joint detection of a quantized two-dimensional Gaussian hidden Markovian source at the receiver, while in [16] only a single Markov source is considered. The paper’s main contributions include modeling the behavior of the correlated sources via a hidden Markov model, verifying the system parameters via simulations, designing a joint sequence MAP decoder (which is optimal in terms of sequence error probability), and implementing it using an appropriately modified version of Viterbi algorithm so that the decoder can take full advantage of the sources’ correlation and temporal memory as well as the channels’ soft-decision information and temporal memory (due to the fading process in each MAC sub-channel) to achieve improved and robust signal-to-distortion ratio (SDR) performance for the overall system. A central contribution is the derivation of easy-to-check closed-form necessary and sufficient conditions in terms of the sources and channel parameters, under which the costly delay-prone joint sequence MAP decoder can be replaced by a straightforward instantaneous (symbol-by-symbol) decoder of identical performance.

The rest of this paper is organized as follows. In Section II, we introduce the source and MAC models. In Section III, we formulate the problem and summarize the paper’s contributions. In Section IV, we design the joint sequence MAP decoder and specify its algorithmic

¹This is in line with the well-known facts that memory increases capacity for a large class of ergodically behaving channels [18], [19] and that the use of soft-decision output information can improve channel capacity vis-a-vis hard-decision [20].

implementation. In Section V, we consider using two-level source quantizers and estimate the quantized sources with a Markov process model. We then establish necessary and sufficient conditions under which the expensive joint MAP decoder reduces to a simple instantaneous decoder without any loss in optimality. In Section VI, we numerically illustrate and validate the derived theoretical results and present the SDR performance of the joint sequence MAP and instantaneous decoders for a variety of system conditions. We show that the MAP JSC decoding scheme can successfully employ the source and channel characteristics and temporal memories in recovering the observed data. Finally, we conclude the paper in Section VII.

II. SOURCE AND CHANNEL MODELS

A. Source Model

We consider two correlated zero-mean and unit-variance Gaussian sources \mathcal{V} and \mathcal{V}' whose correlation coefficient is temporally driven by a Markov chain. Such a source model is motivated by the practical WSN scenario where the correlation between two environmental parameters observed by sensors changes over time according to weather conditions. More specifically, we consider a correlation coefficient process generated via a stationary two-state first-order Markov chain $\{\Phi_i\}_{i=1}^{\infty}$ with alphabet $\{\phi_0, \phi_1\}$ where $-1 \leq \phi_0, \phi_1 \leq 1$. Conditioned on the correlation n -tuple $\Phi^n = (\Phi_1, \Phi_2, \dots, \Phi_n)$ for $n \geq 1$, the two-dimensional source process $\{(V_i, V'_i)\}_{i=1}^{\infty}$ generates a sequence of independent and identically distributed (i.i.d.) sample pairs $(V^n, V'^n) = ((V_1, V'_1), (V_2, V'_2), \dots, (V_n, V'_n))$ under the following joint conditional density

$$f_{V^n, V'^n | \Phi^n}(v^n, v'^n | \phi^n) = \prod_{i=1}^n f_{V, V' | \Phi}(v_i, v'_i | \phi_i), \quad v^n, v'^n \in \mathbb{R}^n, \phi^n \in \{\phi_0, \phi_1\}^n$$

where $f_{V, V' | \Phi}(\cdot, \cdot | \phi)$ is the standard bivariate Gaussian density with correlation coefficient ϕ

$$f_{V, V' | \Phi}(v, v' | \phi) = \frac{1}{2\pi\sqrt{1-\phi^2}} \exp\left(-\frac{v^2 + v'^2 - 2\phi vv'}{2(1-\phi^2)}\right). \quad (1)$$

The Markov process $\{\Phi_i\}_{i=1}^{\infty}$ is governed by the following two-state transition matrix

$$T_{\phi} = \begin{bmatrix} t_{\phi_0\phi_0} & 1 - t_{\phi_0\phi_0} \\ 1 - t_{\phi_1\phi_1} & t_{\phi_1\phi_1} \end{bmatrix}, \quad (2)$$

where $t_{\phi_0\phi_0} \triangleq \Pr\{\Phi_i = \phi_0 | \Phi_{i-1} = \phi_0\}$ and $t_{\phi_1\phi_1} \triangleq \Pr\{\Phi_i = \phi_1 | \Phi_{i-1} = \phi_1\}$ are the probabilities of the correlation coefficient staying in the same state at the current time slot given that the previous time slot state is ϕ_0 and ϕ_1 , respectively. Note that the individual processes $\{V_i\}_{i=1}^{\infty}$ and $\{V'_i\}_{i=1}^{\infty}$ are each i.i.d. Gaussian. However, the two-dimensional source process $\{(V_i, V'_i)\}_{i=1}^{\infty}$, which is a Gaussian mixture process, exhibits temporal memory in the form of a hidden Markov model (HMM) by virtue of the Markov property of the correlation coefficient process.

Special case: If we collapse the alphabet of the correlation coefficient to a single unit-mass point by setting $\phi_0 = \phi_1$, then the coefficient process becomes deterministic and hence constant over time. This renders the process $\{(V_i, V'_i)\}_{i=1}^{\infty}$ memoryless (i.e., i.i.d.) and Gaussian.

B. Channel Model

Before introducing the orthogonal MAC model, we briefly review two point-to-point channel models studied in [17]: the Rayleigh DFC and the NBNDQ-QB. As the NBNDQ-QB is more amenable to system analysis and was shown to effectively represent the statistical behavior of the Rayleigh DFC under various uncoded modulation [17], [30], lossy JSC coding [16] and low-density parity-check channel coding [31] settings, the orthogonal MAC considered in this paper will be composed of two point-to-point NBNDQ-QB sub-channels.

1) *Point-to-Point Rayleigh DFC:* The single-user Rayleigh DFC, which is a well-known model for point-to-point wireless channels, is a binary-input 2^q -ary output channel as shown in Fig. 1.

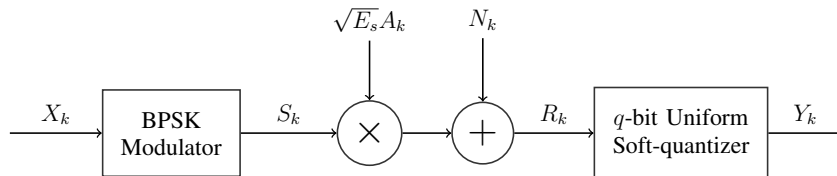


Fig. 1: Rayleigh discrete fading channel (DFC).

First, a binary phase-shift keying (BPSK) modulator takes the DFC's binary input process $\{X_k\}_{k=1}^{\infty}$, $X_k \in \mathcal{X} = \{0, 1\}$, and generates $S_k = 2X_k - 1 \in \{-1, 1\}$ for $k = 1, 2, \dots$. Then, the modulated signal is transmitted over a time-correlated flat Rayleigh fading channel with additive white Gaussian noise which produces the output $R_k = \sqrt{E_s}A_kS_k + N_k, k = 1, 2, \dots$, where E_s is the energy of the signal sent over the channel, and $\{N_k\}$ is a sequence of i.i.d. Gaussian random variables of variance $N_0/2$. Here, $\{A_k\}$ is the channel's fading process (assumed to be independent of $\{N_k\}$ and the input process) with $A_k = |G_k|$, where $\{G_k\}$ is a time-correlated complex wide-sense stationary Gaussian process with Clarke's autocorrelation function given as a Bessel function of the normalized maximum Doppler frequency f_dT [17], [32]. As a result, each fading random variable A_k , which causes an attenuation in the signal, is Rayleigh distributed with unit second moment. Correlation in the fading coefficients $\{A_k\}$ models the channel's temporal memory. The DFC's signal-to-noise ratio (SNR) is given by $\text{SNR} = E_s/N_0$. Finally, a soft-decision demodulator processes the output R_k and produces the DFC's output $Y_k \in \mathcal{Y} = \{0, 1, \dots, 2^q - 1\}$ using a q -bit uniform quantizer with step size Δ defined as $Y_k = j$, if $R_k \in (T'_{j-1}, T'_j]$, where $T'_{-1} = -\infty, T'_j = (j + 1 - 2^{q-1})\Delta$ for $j = 0, 1, \dots, 2^q - 2$, and $T'_{2^q-1} = \infty$.

For the DFC, the probabilities $\Pr\{Y_k = j | X_k = i, A_k = \tilde{a}\}$, $i \in \{0, 1\}$, $j \in \mathcal{Y}$, $\tilde{a} \geq 0$, and the n -fold transition probabilities $P_{DFC}^{(n)}(y_1^n | x_1^n) \triangleq \Pr\{Y_1^n = y_1^n | X_1^n = x_1^n\}$ can be calculated via [17, eqs. (1), (2)] where $y_1^n = (y_1, y_2, \dots, y_n)$ and $x_1^n = (x_1, x_2, \dots, x_n)$. However, $P_{DFC}^{(n)}(y_1^n | x_1^n)$ can only be expressed in closed form for $n \leq 3$ [33], [34]; for $n > 3$, it must be found numerically. Thus, the NBNDQ-QB is introduced as a more tractable model for the DFC.

2) *NBNDQ-QB*: The NBNDQ-QB [17] is a binary-input 2^q -ary-output channel described by

$$Y_k = (2^q - 1)X_k + (-1)^{X_k}Z_k, \quad k = 1, 2, \dots, \quad (3)$$

where $q \geq 1$ is an integer, $X_k \in \{0, 1\}$ is the input data bit, $Y_k \in \mathcal{Y} = \{0, 1, \dots, 2^q - 1\}$ is the channel output, and $Z_k \in \mathcal{Y}$ is the corresponding noise symbol which is assumed to be independent of the input. Here, the noise process is a generalization of the binary queue-based (QB) noise studied in [19]; it is a 2^q -ary stationary ergodic M^{th} -order Markov process which

can be described using only $2^q + 2$ parameters (typically, $q = 2$ or 3 for most systems; hence, the complexity in q is not a concern): the memory order M , the marginal probability distribution $(\rho_0, \rho_1, \dots, \rho_{2^q-1})$, and correlation parameters $0 \leq \epsilon < 1$ and $\alpha \geq 0$. In the special case of $\epsilon = 0$ and $q = 1$, the NBNDC-QB reduces to the familiar memoryless binary symmetric channel. More details on the channel model, including its n -fold transition distribution, are given in [17], [19].

The NBNDC-QB can be fitted, via the modeling procedure explained in [17, Sec. V], to mimic the statistical behavior² of a given Rayleigh DFC with fixed parameters (SNR, q , δ , $f_D T$). The QB memory and correlation parameters M , ϵ and α are coupled with $f_D T$, while the QB noise one-dimensional probability distributions ρ_j for $j \in \mathcal{Y}$ can be determined using the DFC's parameters q , δ and SNR as given in [16, Table I] (see also [36, Section 2.1.2]). Consequently, both models will have the same channel noise correlation coefficient, Cor , given in [17, eq. (22)]. Note that the NBNDC-QB model (and its simpler binary-noise version) has been validated as an effective approximation of the Rayleigh DFC in terms of codeword error rate or SDR fidelity for various coded point-to-point systems [16], [31], [35].

3) *Orthogonal MAC*: In many practical communication systems where the available channel bandwidth must be efficiently shared among several users, various orthogonal multiple access schemes such as frequency division multiple access, time division multiple access, and code division multiple access are employed to avoid unrecoverable collision of messages from different users. This motivates us to consider an orthogonal MAC consisting of two independent single-user Rayleigh DFC sub-channels which are modeled via NBNDC-QB channels.

III. PROBLEM FORMULATION AND SUMMARY OF CONTRIBUTIONS

In Fig. 2, we depict our two-user communication system, referred to as SQ-MAC-MAP system, which generalizes the single-user system studied in [16].

The output samples v of the first source are encoded using a rate- n scalar quantizer (SQ). Although, having a simple SQ instead of a more powerful vector quantizer is dictated by

²It is shown in [17, Sec. II.B] that the DFC can be mathematically expressed via the NBNDC with an ergodic noise process. Given that this noise process has infinite memory, it is then approximated via the M^{th} -order QB Markov noise process [17, Sec. IV] (where the approximation is validated in terms of noise autocorrelation function and channel capacity), resulting in the NBNDC-QB model for the DFC.

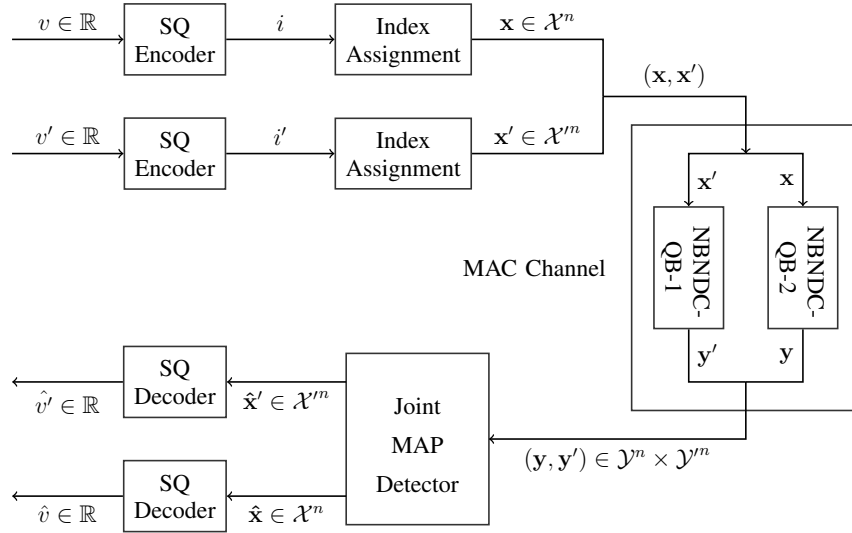


Fig. 2: Two-user system with scalar quantization and joint MAP decoding over an orthogonal MAC with memory.

the limitation of the sensors, this coding method will preserve more redundancy in the index codewords at the quantizer output, which can be later used, in conjunction with channel's characteristics, by the joint MAP decoder for the purpose of robust error correction. The SQ is designed utilizing the Lloyd-Max algorithm [37], with the initial codebook selection obtained via the splitting algorithm [38] and it produces an index $i \in \{0, 1, \dots, 2^n - 1\}$. As explained in [16], because of its simplicity and good performance, the folded binary code (FBC) [9] is chosen as the one-to-one index assignment method to map the index i to a binary vector $\mathbf{x} \in \{0, 1\}^n$. The same encoding process is separately done for the second source which results in the codeword $\mathbf{x}' \in \{0, 1\}^n$. Then, the vector pair $(\mathbf{x}, \mathbf{x}')$ is transmitted through the orthogonal Rayleigh DFC MAC (with its NBND-C-QB sub-channels) and the corresponding vectors $\mathbf{y} \in \mathcal{Y}^n = \{0, 1, \dots, 2^q - 1\}^n$ and $\mathbf{y}' \in \mathcal{Y}'^n = \{0, 1, \dots, 2^{q'} - 1\}^n$ are received. This communication is modeled as bit-by-bit sending of the n -tuple codeword \mathbf{x} over the first NBND-C-QB sub-channel with 2^q -ary noise symbols $z \in \mathcal{Y} = \{0, 1, \dots, 2^q - 1\}$ and noise memory M which will result in the output sequence \mathbf{y} . Similarly, \mathbf{x}' and \mathbf{y}' are the input and output vectors of the second NBND-C-QB sub-channel with $2^{q'}$ -ary noise symbols $z' \in \mathcal{Y}' = \{0, 1, \dots, 2^{q'} - 1\}$ and noise memory M' . At the receiver side, the MAC's output $(\mathbf{y}, \mathbf{y}')$ is fed to a joint MAP decoder. Finally, two SQ decoders map the decoder outputs $(\hat{\mathbf{x}}, \hat{\mathbf{x}}')$ into the source estimates

(v, \hat{v}) . Note that in this system, the receiver carries most of the complexity load; hence it is specially suitable to WSN applications.

The main contributions of this work are summarized as follows.

- Approximate the paired sequence of the quantized sources via a Markov process, design a joint sequence MAP decoder which is optimal in terms of the joint sequence error probability, and implement it via a properly modified version of the Viterbi algorithm [39].
- Analyze the case when the sources are binary-quantized and derive the statistical properties of the Markov process representing the paired sequence of the quantized sources (Lemma 1).
- Establish for the above binary quantization case necessary and sufficient conditions (Theorem 1) under which the delay-prone joint sequence MAP decoder can be replaced without sacrificing optimality with a delayless symbol-by-symbol decoder (analyzed in Lemma 2).
- Validate the analytical results numerically and show via simulations the benefits of MAP decoding in the SQ-MAC-MAP system as it judiciously harnesses the sources' residual redundancy as well as the sub-channels' noise correlation and soft-decision information.

IV. JOINT SEQUENCE MAP DECODING FOR THE TWO-USER MAC SYSTEM

The residual redundancy of the sources (post quantization) and the channel statistics can be exploited by a MAP decoder which is designed to minimize the sequence error probability. Suppose that each source produces N symbols. The sequence $(\mathbf{x}, \mathbf{x}')^N = ((\mathbf{x}_1, \mathbf{x}'_1), \dots, (\mathbf{x}_N, \mathbf{x}'_N)) \in (\{0, 1\} \times \{0, 1\})^{nN}$ at the output of the SQ encoders is transmitted over the MAC in nN channel uses. The independent NBNDQ-QB sub-channels contaminate the bit streams related to the first and second source with noise sequences $z_1^{nN} \in \mathcal{Y}^{nN}$ and $z_1'^{nN} \in \mathcal{Y}'^{nN}$, respectively. In other words, the input n -tuples \mathbf{x}_{i+1} and \mathbf{x}'_{i+1} , $i = 0, 1, \dots, N - 1$, are bit-by-bit transmitted over the first and second sub-channels with the corresponding noise symbols $(z_{ni+1}, z_{ni+2}, \dots, z_{n(i+1)})$ and $(z'_{ni+1}, z'_{ni+2}, \dots, z'_{n(i+1)})$ which will result in the output n -tuples \mathbf{y}_{i+1} and \mathbf{y}'_{i+1} .

Given that the source $\{(V_i, V'_i)\}_{i=1}^\infty$ is an HMM, the resulting process produced by the quantizers does not admit a closed-form expression for its block distribution; this makes implementing the sequence MAP decoder based on the Viterbi algorithm quite complicated and computa-

tionally expensive. Hence, we model this process via a stationary first-order Markov process $\{(X_i, X'_i)\}_{i=1}^{\infty}$. For $(\mathbf{x}_1, \mathbf{x}'_1) \in (\{0, 1\} \times \{0, 1\})^n$, let $\pi(\mathbf{x}_1, \mathbf{x}'_1) \triangleq \Pr\{(\mathbf{X}_1, \mathbf{X}'_1) = (\mathbf{x}_1, \mathbf{x}'_1)\}$ be the stationary joint distribution corresponding to the approximated first-order Markov model and let $P((\mathbf{x}_{i+1}, \mathbf{x}'_{i+1}) | (\mathbf{x}_i, \mathbf{x}'_i)) \triangleq \Pr\{(\mathbf{X}_{i+1}, \mathbf{X}'_{i+1}) = (\mathbf{x}_{i+1}, \mathbf{x}'_{i+1}) | (\mathbf{X}_i, \mathbf{X}'_i) = (\mathbf{x}_i, \mathbf{x}'_i)\}$ denote the transition probabilities.³

Assuming $nN \geq \max\{M, M'\}$, where M and M' are the noise memory orders of the corresponding sub-channels, the sequence MAP decoder receives the channel output $(\mathbf{y}, \mathbf{y}')^N = ((\mathbf{y}_1, \mathbf{y}'_1), \dots, (\mathbf{y}_N, \mathbf{y}'_N)) \in (\mathcal{Y} \times \mathcal{Y}')^{nN}$, and estimates $(\mathbf{x}, \mathbf{x}')^N \in (\{0, 1\} \times \{0, 1\})^{nN}$ by $(\hat{\mathbf{x}}, \hat{\mathbf{x}}')^N$ given by

$$\begin{aligned} (\hat{\mathbf{x}}, \hat{\mathbf{x}}')^N &= \arg \max_{\mathbf{x}, \mathbf{x}'^N} \Pr\{(\mathbf{X}, \mathbf{X}')^N = (\mathbf{x}, \mathbf{x}')^N | (\mathbf{Y}, \mathbf{Y}')^N = (\mathbf{y}, \mathbf{y}')^N\} = \\ & \arg \max_{(\mathbf{x}, \mathbf{x}')^N} \left\{ \log [P_{QB}^{(n)}(z_1^n) P'_{QB}{}^{(n)}(z'_1{}^n) \pi(\mathbf{x}_1, \mathbf{x}'_1)] + \right. \\ & \left. \sum_{i=1}^{N-1} \log \left[Q(z_{in+1}^{(i+1)n} | z_{in-(M-1)}^{in}) \times Q'(z'_{in+1}{}^{(i+1)n} | z'_{in-(M'-1)}{}^{in}) \times P((\mathbf{x}_{i+1}, \mathbf{x}'_{i+1}) | (\mathbf{x}_i, \mathbf{x}'_i)) \right] \right\}, \end{aligned} \quad (4)$$

For $i = 1, 2, \dots, nN$, the noise symbols z_i and z'_i can be found by separately substituting each sub-channel input and output into (3). For the first sub-channel, the n -fold channel transition probabilities are $\Pr\{Z_1^n = z_1^n\} = \Pr\{Y_1^n = y_1^n | X_1^n = x_1^n\} \triangleq P_{QB}^{(n)}(z_1^n)$, as given by [17, eqs. (20), (21)], where y_1^n is the output sequence, x_1^n the input sequence, and $z_1^n = (z_1, \dots, z_n)$ is the sequence of corresponding noise symbols related to x_1^n and y_1^n according to (3). For $n = 1$, $P_{QB}^{(1)}(z_1) = \rho_{z_1}$ for all $z_1 \in \mathcal{Y}$.

The noise transition probabilities $Q(z_{in+1}^{(i+1)n} | z_{in-(M-1)}^{in})$ are defined based on $Q(z_{i+1}^{i+j} | z_{i-k}^j) \triangleq \Pr\{Z_{i+1}^{i+j} = z_{i+1}^{i+j} | Z_{i-k}^j = z_{i-k}^j\}$, where $i, j, k \in \{1, 2, \dots, nN - 1\}$, $i + j \leq nN$, $i - k \geq 1$. Note that $z_i \triangleq 0$ if $i < 1$, $z_i^j \triangleq (z_i, z_{i+1}, \dots, z_j)$, $j \geq i$. They can be computed via [17]. For the second sub-channel, $Q'(z'_{in+1}{}^{(i+1)n} | z'_{in-(M'-1)}{}^{in})$ and $P'_{QB}{}^{(n)}(z'_1{}^n)$ are defined and calculated similarly using the parameters associated with this channel. The step-by-step details of how (4) is derived, by

³Note that in all simulations, the actual HMM source is generated while the decoder uses the statistics of the approximating Markov source which are empirically estimated for $n > 1$ (for $n = 1$, they can be exactly determined as shown in Lemma 1).

using the Bayes rule and the orthogonality of the sub-channels, can be found in [36, Sec. 3.2].

To implement the MAP decoder, we employ a modified version of the Viterbi algorithm by properly extending the one used in [40] to our two-user system. The corresponding trellis consists of $4^{(kn)}$ states, the set of all possible pairs of kn -tuple codewords, where k is the smallest integer which satisfies $kn \geq \max\{M, M'\}$. In the trellis, each state has $2^{(kn-M+1)} \times 2^{(kn-M'+1)}$ incoming and 4^n outgoing branches and the path metric at step i is as follows:

$$\log [Q(z_{in+1}^{(i+1)n} | z_{in-(M-1)}^{in})Q'(z'_{in+1}{}^{(i+1)n} | z'_{in-(M'-1)}{}^{in})] + \log [P((\mathbf{x}_{i+1}, \mathbf{x}'_{i+1}) | (\mathbf{x}_i, \mathbf{x}'_i))].$$

Applying the Viterbi algorithm, the MAP decoder needs to observe the entire received sequence before deciding on the most likely message words, which results in significant decoding delay as well as storage complexity of order $\mathcal{O}(nN4^{(kn)})$ that increases with the length of the sequence. Thus it is interesting to investigate situations where MAP decoding can be replaced by a simple and fast instantaneous (symbol-by-symbol) decoding rule which exhibits the same performance in terms of symbol error rate (SER).

V. CASE STUDY: JOINT MAP DETECTION OF BINARY MARKOV CORRELATED SOURCES

In this section, we mathematically study the joint sequence MAP detection problem when the sources are binary-quantized. We first approximate the stream of pairs of bits after quantization, which forms an HMM process, via a Markov process (having the same second-order statistics as the underlying HMM), study its properties, and derive its statistics. We then introduce the instantaneous joint symbol-by-symbol decoder and analyze it. Finally, we establish necessary and sufficient conditions for the equivalence between the delay-prone joint sequence MAP decoder and the instantaneous (zero delay) symbol-by-symbol decoder that causes no loss in optimality in terms of minimizing the joint sequence error probability.

A. Markov Modeling of the Binary-Quantized Sources

Under two-level quantization (with $n = 1$ and a quantization threshold set at zero), the resulting joint process $\{(X_n, X'_n)\}_{n=1}^{\infty}$ having alphabet $\{0, 1\}^2 = \{00, 01, 10, 11\}$ is hidden

Markov, governed by the Markov process $\{\Phi_n\}$ described by (2). To facilitate the analysis, as described in Section IV, we model $\{(X_n, X'_n)\}_{n=1}^\infty$ as a stationary first-order Markov process by matching its second-order distribution to that of the underlying HMM source whose probability measure is denoted by P_{HMM} .

Lemma 1. The transition matrix of the Markov source $\{(X_n, X'_n)\}$ is given by

$$T = \begin{bmatrix} P_{00-00} & P_{00-01} & P_{00-10} & P_{00-11} \\ P_{01-00} & P_{01-01} & P_{01-10} & P_{01-11} \\ P_{10-00} & P_{10-01} & P_{10-10} & P_{10-11} \\ P_{11-00} & P_{11-01} & P_{11-10} & P_{11-11} \end{bmatrix} = \begin{bmatrix} a & b & b & a \\ c & d & d & c \\ c & d & d & c \\ a & b & b & a \end{bmatrix}, \quad (5)$$

where $P_{jk-lm} \triangleq \Pr\{(X_i, X'_i) = (l, m) | (X_{i-1}, X'_{i-1}) = (j, k)\}$ for $j, k, l, m \in \{0, 1\}$, and the probabilities a, b, c and d are given in terms of the statistics of the underlying HMM source $\{(V_i, V'_i)\}$ as follows:

$$\begin{aligned} a &= \frac{a'[a't_{\phi_0\phi_0}P_{\phi_0} + c'(1 - t_{\phi_1\phi_1})(1 - P_{\phi_0})] + c'[a'(1 - t_{\phi_0\phi_0})P_{\phi_0} + c't_{\phi_1\phi_1}(1 - P_{\phi_0})]}{a'P_{\phi_0} + c'(1 - P_{\phi_0})}, \\ b &= \frac{b'[a't_{\phi_0\phi_0}P_{\phi_0} + c'(1 - t_{\phi_1\phi_1})(1 - P_{\phi_0})] + d'[a'(1 - t_{\phi_0\phi_0})P_{\phi_0} + c't_{\phi_1\phi_1}(1 - P_{\phi_0})]}{a'P_{\phi_0} + c'(1 - P_{\phi_0})}, \\ c &= \frac{a'[b't_{\phi_0\phi_0}P_{\phi_0} + d'(1 - t_{\phi_1\phi_1})(1 - P_{\phi_0})] + c'[b'(1 - t_{\phi_0\phi_0})P_{\phi_0} + d't_{\phi_1\phi_1}(1 - P_{\phi_0})]}{b'P_{\phi_0} + d'(1 - P_{\phi_0})}, \\ d &= \frac{b'[b't_{\phi_0\phi_0}P_{\phi_0} + d'(1 - t_{\phi_1\phi_1})(1 - P_{\phi_0})] + d'[b'(1 - t_{\phi_0\phi_0})P_{\phi_0} + d't_{\phi_1\phi_1}(1 - P_{\phi_0})]}{b'P_{\phi_0} + d'(1 - P_{\phi_0})}, \end{aligned}$$

where $P_{\phi_0} \triangleq \Pr\{\Phi_i = \phi_0\} = 1 - \Pr\{\Phi_i = \phi_1\} = \frac{1 - t_{\phi_1\phi_1}}{2 - (t_{\phi_0\phi_0} + t_{\phi_1\phi_1})}$ is the stationary distribution of the Markov process $\{\Phi_i\}_{i=1}^\infty$, and

$$\begin{aligned} a' &\triangleq P_{\text{HMM}}\{(X_i, X'_i) = (0, 0) | \Phi_i = \phi_0\} = \Pr\{V < 0, V' < 0 | \Phi = \phi_0\} \\ b' &\triangleq P_{\text{HMM}}\{(X_i, X'_i) = (0, 1) | \Phi_i = \phi_0\} = \Pr\{V < 0, V' \geq 0 | \Phi = \phi_0\} \\ c' &\triangleq P_{\text{HMM}}\{(X_i, X'_i) = (0, 0) | \Phi_i = \phi_1\} = \Pr\{V < 0, V' < 0 | \Phi = \phi_1\} \\ d' &\triangleq P_{\text{HMM}}\{(X_i, X'_i) = (0, 1) | \Phi_i = \phi_1\} = \Pr\{V < 0, V' \geq 0 | \Phi = \phi_1\} \end{aligned} \quad (6)$$

which can be calculated using the bivariate Gaussian distribution (1).

Proof of Lemma 1. The proof is given in Appendix A. ■

Note that since T is a stochastic matrix, we get that $a + b = c + d = 1/2$. The Markov source's stationary distribution vector, denoted by $\pi = [P(0, 0), P(0, 1), P(1, 0), P(1, 1)]$, where $P(x, x') \triangleq \Pr\{(X, X') = (x, x')\}$, has the following components

$$P(0, 0) = P(1, 1) = \frac{c}{1 + 2(c - a)}; \quad P(1, 0) = P(0, 1) = \frac{1}{2} - P(0, 0) = \frac{1 - 2a}{2(1 + 2(c - a))}. \quad (7)$$

B. Instantaneous Symbol-by-Symbol Decoder

We next present a simple instantaneous symbol-by-symbol decoder. Specifically, by making use of (7), the orthogonality of the MAC, and an ordering assumption on the marginal probabilities of each NBNDQ-QB sub-channel, we shown in Lemma 2 that among all mappings $\theta : \mathcal{Y} \mapsto \{0, 1\}$, the following mapping θ^* minimizes the bit error probability for each source:

$$\theta^*(y) = \tilde{y} = \begin{cases} 0, & \text{if } y < 2^{q-1} \\ 1, & \text{otherwise.} \end{cases} \quad (8)$$

Note that we independently apply the same function (8) to y and y' , the outputs of the orthogonal MAC, and acquire binary symbols \tilde{y} and \tilde{y}' , respectively. Since the parameters of the NBNDQ-QB's can be different, we denote the first instantaneous decoder by θ^* and the second by θ'^* with the q in (8) changed to q' . Hence, when the sent pair (x, x') is received as (y, y') at the MAC output, the decoder pair (θ^*, θ'^*) jointly decodes correctly if $(\tilde{y}, \tilde{y}') = (x, x')$.

Lemma 2. Let N -sequences of the above Markov source $\{(X_n, X'_n)\}$ described by (5) and (7) be sent over the orthogonal MAC consisting of two independent NBNDQ-QB sub-channels as described in Section II-B and assume that the output sequences are instantaneously decoded as $(\tilde{y}, \tilde{y}')^N = (\theta^*(y), \theta'^*(y'))^N$, where the mapping pair (θ^*, θ'^*) described above is applied component-wise to each output pair (y_i, y'_i) , $i = 1, \dots, N$.

If the first NBNDQ-QB sub-channel has noise parameters satisfying $\rho_0 \geq \rho_1 \geq \dots \geq \rho_{2^q-1}$, then among all mappings $\theta : \mathcal{Y} \mapsto \{0, 1\}$, where $\mathcal{Y} = \{0, 1, \dots, 2^q - 1\}$, the mapping θ^* as given

by (8) yields the lowest bit error probability defined as $\Pr\{\tilde{Y} \neq X\}$. The same result also holds for the the second NBNDC-QB sub-channel and source $\{X'_n\}$, with the optimal function θ'^* given as in (8) with q' replacing q .

Proof of Lemma 2. The proof of this lemma which extends [16, Lemma 1] from the single to the two user setting can be found in [36, Lemma 3.1]. ■

Remark: Observe that while θ^* and θ'^* separately minimize the bit error probability of the individual sources $\{X_n\}$ and $\{X'_n\}$, respectively, they do not necessarily minimize the joint symbol error probability of $\{(X_n, X'_n)\}$. Note also that when $q = q' = 1$, the binary output sequences can be accepted without any further processing by the decoder; this is known in the literature as “decode-what-you-see” or “singlet decoding” (e.g., see [23], [28]).

C. Equivalence Between Joint Sequence MAP Decoding and Instantaneous Decoding

The following main result presents a necessary and sufficient condition for the mapping pair (θ^*, θ'^*) to form an optimal sequence detection rule in the sense of minimizing the sequence error probability. In this case, the MAP decoder is unnecessary and can be replaced by the instantaneous decoders (θ^*, θ'^*) , without increasing the error probability.

Theorem 1. Consider the first-order Markov source $\{(X_i, X'_i)\}_{i=1}^\infty$ described by (5) and (7). Consider also the orthogonal MAC with two independent NBNDC-QB sub-channels: one sub-channel with correlation parameters $\epsilon \geq 0$ and $\alpha = 1$, memory order $M = 1$, $q \geq 1$, and noise one-dimensional probability distribution satisfying $\rho_0 \geq \rho_1 \geq \dots \geq \rho_{2q-1}$, and the other sub-channel with parameters $\epsilon' \geq 0$, $q' \geq 1$, $M' = \alpha' = 1$, and $\rho'_0 \geq \rho'_1 \geq \dots \geq \rho'_{2q'-1}$. Let $(x, x')^N$ be a source sequence of length $N \geq 2$, let $(y, y')^N$ be the channel output sequence, and let $(\tilde{y}, \tilde{y}')^N = (\theta^*(y), \theta'^*(y'))^N$ be the sequence obtained by applying the instantaneous decoders (θ^*, θ'^*) component-wise to $(y, y')^N$.

Sufficient Condition: Assuming $(x_1, x'_1) = (\tilde{y}_1, \tilde{y}'_1)$, we have that $(\hat{x}, \hat{x}')^N = (\tilde{y}, \tilde{y}')^N$ is an optimal

sequence MAP detection rule for all possible received sequences if

$$A \times \left(\min \left\{ \frac{a}{b}, \frac{b}{a}, \frac{c}{d}, \frac{d}{c} \right\} \times \min \left\{ \frac{a}{c}, \frac{b}{d}, \frac{d}{b}, \frac{c}{a} \right\} \right) \geq 1, \quad (9)$$

where

$$A = \min \left\{ \frac{\epsilon' + (1 - \epsilon')\rho'_{2^{q'}-1-1}}{\epsilon' + (1 - \epsilon')\rho'_{2^{q'}-1}}, \frac{\epsilon + (1 - \epsilon)\rho_{2^q-1-1}}{\epsilon + (1 - \epsilon)\rho_{2^q-1}} \right\}, \quad (10)$$

and a , b , c , and d are the source transition probabilities defined in (5).

Necessary Conditions: Conversely, a necessary condition for the joint MAP decoder to be unnecessary is given by

$$\min \left\{ \frac{\rho_{2^q-1-1}}{\rho_{2^q-1}}, \frac{\rho'_{2^{q'}-1-1}}{\rho'_{2^{q'}-1}} \right\} \times \min \left\{ \frac{a}{b}, \frac{b}{a}, \frac{c}{d}, \frac{d}{c} \right\} \geq 1. \quad (11)$$

In other words, if (11) does not hold, then there is at least one pair of input and output sequences of length $N \geq 2$ for which $(\hat{x}, \hat{x}')^N = (\tilde{y}, \tilde{y}')^N$ is not an optimal sequence MAP detection rule (this condition has no dependence on the sub-channels noise correlations ϵ and ϵ').

Furthermore for a large enough N , a necessary condition that is tighter than (11) is given by

$$\min \left\{ A \min \left\{ \frac{a}{d}, \frac{d}{a} \right\}, \min \left\{ \frac{\rho_{2^q-1-1}}{\rho_{2^q-1}}, \frac{\rho'_{2^{q'}-1-1}}{\rho'_{2^{q'}-1}} \right\} \times \min \left\{ \frac{a^2}{bc}, \frac{bc}{a^2}, \frac{bc}{d^2}, \frac{d^2}{bc} \right\} \right\} \geq 1. \quad (12)$$

Proof. See Appendix B. □

Remark: It is worth pointing out that the main result of [1] is a special case of Theorem 1 above: when the source $\{(X_i, X'_i)\}_{i=1}^{\infty}$ is memoryless in time (which can be realized by setting $\phi_0 = \phi_1$ in the source statistics, see Section II-A), then the necessary and sufficient conditions of Theorem 1 directly reduce to the ones in [1, Theorem 1], see [36, Sec. 4.3.1] for details.

VI. SIMULATION RESULTS

A. Validation of Theorem 1

We illustrate and validate Theorem 1 in Figs. 4-5 and Tables I-II under various source and MAC sub-channels conditions. The system was simulated using two correlated binary input sequences of length $N = 10^5$, which are jointly generated according to the first-order Markov

process $\{(X_i, X'_i)\}$ with transition matrix (5). As explained in Section V, this Markov process is an approximation (with matching second-order statistics) of the process resulting from the binary-quantization (with $n = 1$) of the bivariate Gaussian HMM $\{(V_i, V'_i)\}$ driven by the Markov correlation coefficient process $\{\Phi_i\}_{i=1}^{\infty}$ with transition matrix (2). The MAC's NBNDCC-QB sub-channels are simulated under similar conditions as in [16]. Each simulation is repeated 10 times and the average joint symbol error rate is computed to ensure the results are consistent. It is important to mention that the assumption on (x_1, x'_1) in Theorem 1 was not enforced in the simulations; yet the simulations indicate that the theorem's result holds without this assumption. Furthermore, we define an average correlation coefficient for the $\{(V_i, V'_i)\}$ source as

$$\phi_{\text{av}} = P_{\phi_0} \times \phi_0 + (1 - P_{\phi_0}) \times \phi_1, \quad (13)$$

where $P_{\phi_0} = \frac{1 - t_{\phi_1\phi_1}}{2 - (t_{\phi_1\phi_1} + t_{\phi_0\phi_0})}$ is the stationary distribution of the Markov process $\{\Phi_i\}$. The numerical results show that ϕ_{av} can be a good measure for evaluating the combined effect of the correlation between V_i and V'_i and the temporal memory in $\{(V_i, V'_i)\}$. Hence, we use ϕ_{av} to address different source conditions in the simulations.

We consider several scenarios in generating $\{(X_i, X'_i)\}$. In Table I and Figs. 4-5, we choose the parameters in the matrix (5) as $a = 0.28, b = 0.22, c = 0.33, d = 0.17$, which represent an underlying HMM with parameters $\phi_0 = -0.31, \phi_1 = 0.81, t_{\phi_0\phi_0} = t_{\phi_1\phi_1} = 0.2$; for this case, $\phi_{\text{av}} = 0.25$. We also use the parameters $a = 0.36, b = 0.14, c = 0.37, d = 0.13$, yielding an underlying HMM with $\phi_0 = -0.31, \phi_1 = 0.81, (t_{\phi_0\phi_0}, t_{\phi_1\phi_1}) = (0.1, 0.8)$; in this case, $\phi_{\text{av}} = 0.61$. Finally, in Table II, we use $a = d = 0.23, b = c = 0.27$ in order to further illustrate Theorem 1. In this case, the underlying HMM has $\phi_0 = -0.5, \phi_1 = 0.5, (t_{\phi_0\phi_0}, t_{\phi_1\phi_1}) = (0.2, 0.2)$, resulting in $\phi_{\text{av}} = 0.0$.

Denoting the left hand term of (9) and (11) by C and C' , respectively, it can be observed from Figs. 4-5 and Tables I-II that when $C \geq 1$ and consequently $C' \geq 1$, the performance of the instantaneous joint decoder (θ^*, θ'^*) and the joint MAP decoder are identical, while for $C' < 1$, implying $C < 1$, the joint MAP decoder can outperform the instantaneous decoder. There is another possible situation where $C < 1$ and $C' \geq 1$; for this case, the instantaneous decoder can

still achieve the same performance as the joint MAP decoder.

The numerical results presented here are only a subset of [36, Tables 3.1- 3.3] where Theorem 1 is illustrated under various source and sub-channels conditions. By scrutinizing all the results, the following observations can be made.

- The joint SER of the instantaneous decoder (θ^*, θ'^*) , while increasing for noisier channels, does not change significantly with (q, q') , (Cor, Cor') , and ϕ_{av} . This behavior can be inferred by examining the SER definition, using (8) and noting that $\rho_0 + \dots + \rho_{2^q-1-1} = \rho_{2^q-1} + \dots + \rho_{2^q}$ for the marginal distributions given in [16, Table I].
- In general, the joint SER of the MAP decoder improves when the parameters (q, q') , (Cor, Cor') , (SNR, SNR') , and ϕ_{av} are increased. Indeed, the results show that (q, q') , (Cor, Cor') , and ϕ_{av} constructively contribute in helping the joint MAP decoder to combat channel errors; i.e., each individual parameter is more effective in the presence of the other parameters having high values. Furthermore, increasing these parameters causes more significant improvements for the sub-channels with low SNR. On the other hand, the SER improvement with increasing (SNR, SNR') is more visible when the parameters (q, q') , (Cor, Cor') , and ϕ_{av} are small.
- When $SNR \leq SNR'$, it is usually more beneficial, in terms of the joint MAP SER improvement, to increase q instead of q' . However, when the sources are not highly correlated and the sub-channels have $Cor < Cor'$, increasing q' results in slightly better results.
- Having sub-channels with $Cor < Cor'$, increasing SNR rather than SNR' has more significant effect on improving the joint SER. When $Cor = Cor'$, improving the SNR of the sub-channel with less resolution leads to better results. Furthermore, the joint SER improvement is more visible when two sources are highly correlated.
- Under the same sub-channels conditions, i.i.d. correlated sources with correlation parameter $\phi_{av} = 0$ result in a better performance, in the terms of SER and SDR, compared to when the correlated Markov sources with $\phi_{av} < \phi_0$ are sent over the channel. For example, comparing Tables 3.5 and 4.5 in [36], it can be observed that the SDR results for i.i.d. correlated sources with $\phi_0 = 0.81$ are always better than the case of correlated Markov

sources with $\phi_{av} = 0.61$. This verifies that ϕ_{av} efficiently represents the total redundancy (in terms of memory and non-uniform distribution) in the sources and provides a means for comparison between different source models.

B. SQ-MAC-MAP System Simulation

We next simulate the SQ-MAC-MAP system for hidden Markov correlated Gaussian sources $\{(V_i, V'_i)\}$. First, the SQ is designed and the distributions $P(x, x')$ and $P_{j_k-l_m}$ are calculated for $n > 1$ using a training set of 10^6 paired source symbols (for $n = 1$, they can be directly determined as shown in Section V-A). Then, 10^5 source symbols are transmitted for simulation and the average SDR with the mean square error (MSE) distortion is measured after repeating each simulation 10 times (for getting consistent results). It is important to point out that the SQ-MAC-MAP scheme is designed to minimize the joint sequence error probability between the SQ encoder output sequences and the SQ decoder input sequences, while we evaluate the system's end-to-end performance in terms of SDR with the MSE distortion measure. Hence, the SQ-MAC-MAP is not necessarily optimal in terms of achieving minimum MSE.⁴ However, we note from the simulations that our system improves SDR performance by exploiting residual source redundancy as well as noise correlation and soft-decision information of the NBNDC sub-channels. Typical simulation results in terms of SDR (in dB) under MAP and instantaneous decoding are shown in Tables III and IV, respectively, where SDR is defined as

$$SDR \triangleq \frac{E[(V)^2] + E[(V')^2]}{E[(V - \hat{V})^2] + E[(V' - \hat{V}')^2]}. \quad (14)$$

Additional results, including the case when the source $\{V_i, V'_i\}$ is i.i.d. (i.e., when setting $\phi_0 = \phi_1$), can be found in [1], [36]. We can observe that the joint MAP decoder successfully takes advantage of the redundancies and statistics of the sources with $\phi_{av} < \phi_0$, of the sub-channels' noise memory and soft-decision resolution. In general, the system performs better when these factors take higher values. However, there are some cases where increasing ϕ_{av} or the sub-

⁴MSE optimal and suboptimal sequential decoders are studied, among others, in [24], [25]. However, to implement MSE optimal decoding in our system would significantly increase the system complexity.

channels' noise correlation does not improve the system SDR (sometimes even worsening it). This phenomenon for $n = 1$ can be explained by rewriting the sufficient condition (9) as

$$\max\{Cor, Cor'\} \leq \min \left\{ \frac{\rho_{2^{q-1}} - B\rho_{2^{q-1}-1}}{B(1 - \rho_{2^{q-1}-1}) + \rho_{2^{q-1}} - 1}, \frac{\rho'_{2^{q'-1}} - B\rho'_{2^{q'-1}-1}}{B(1 - \rho'_{2^{q'-1}-1}) + \rho'_{2^{q'-1}} - 1} \right\}, \quad (15)$$

where

$$B = \min \left\{ \frac{a}{b}, \frac{b}{a}, \frac{c}{d}, \frac{d}{c} \right\} \times \min \left\{ \frac{a}{c}, \frac{b}{d}, \frac{d}{b}, \frac{c}{a} \right\}. \quad (16)$$

In fact, when the sufficient condition (9) holds for two sets of source-channel parameters with the same fixed SNR (where the parameters Cor , ϕ_{av} , and q might vary), the SDR performance of the joint MAP decoder is identical to the SDR performance of the instantaneous decoder which does not change under these two sets of parameters. As shown in Fig. 6, these results also verify that modeling the quantized sources with the first-order Markov source $\{(X_n, X'_n)\}$ is a good approximation, since the input sequences for the simulations illustrating the theorem are generated by the Markov source while the system simulation results are based on the quantizing the original real-valued sources.

Overall, the MAP decoder can realize significant SDR gains by exploiting the source and channel characteristics. From Table III, we note that when $\phi_{av} = 0.61$, SNR= 2 dB and $q = n = 3$, more than 5 dB SDR gain is achieved when the MAP decoder fully exploits the channels' memory with high noise correlation ($Cor = Cor' = 0.9$) over the case of ignoring it by fully interleaving the NBNDC-QB channels ($Cor = Cor' = 0$). Furthermore, we note that incorporating more channel soft-decision information has a positive effect on the performance; e.g., using a 3-bit soft-decision quantizer rather a hard-decision quantizer ($q = 1$) results in a 3.5 dB gain (at $n = 3$, SNR= 2 dB, $Cor = Cor' = 0.9$ and $\phi_{ave} = 0.61$). Similar gains can be obtained when $\{V_i, V'_i\}$ is memoryless, see [1], [36].

From Table IV, we note that increasing the sub-channels' soft-decision resolution and also the correlation between the sources do not have any significant effect on the performance of the instantaneous decoder. These results are predictable because according to (8), for $0 \leq i \leq N$, the outputs of the instantaneous symbol-by-symbol decoder $(\theta^*(y_i), \theta'^*(y'_i))$ can be written as

functions of R_i and R'_i , the unquantized outputs of the Rayleigh fading underlying sub-channels, as follows

$$\tilde{y}_i = \begin{cases} 0, & \text{if } R_i \leq 0 \\ 1, & \text{otherwise} \end{cases}, \quad \tilde{y}'_i = \begin{cases} 0, & \text{if } R'_i \leq 0 \\ 1, & \text{otherwise} \end{cases}, \quad (17)$$

which shows no dependence on q , q' , and $P(x, x')$.

The joint SDR (for both the joint MAP decoder and the joint symbol-by-symbol decoder) of a system with 2-level quantizers ($n = 1$) shows the same behavior as its joint SER which we examined in the previous sub-section. It is observed in [36] that all the arguments regarding the joint MAP SER of the binary input system also hold for the joint MAP SDR of a system with more quantizer levels (e.g., $n = 2$). Unlike the system with binary sources, the SDR results of the instantaneous decoder improve when the noise correlations are increased. Intuitively, this is due to having symbols which consist of n bits ($n > 1$) and have higher probability of being received correctly because of the correlation between the bits. It is also observed that increasing the noise correlation in the sub-channel with lower SNR results in a more significant SDR improvement.

Finally in Fig. 7, we compare the SDR performance of the SQ-MAC-MAP system under joint MAP decoding with that of the system using independently designed individual MAP decoders for each user. We note that significant performance improvements of up to 3.5 dB can be achieved by using the joint MAP decoder.

VII. CONCLUSION AND FUTURE WORK

In this work, we studied a sensor network with two sensors measuring and transmitting information (modeled as two correlated Gaussian sources which are scalar quantized) through an orthogonal Rayleigh DFC MAC (modeled with two independent NBNDQ-QB sub-channels) to a base station, where a joint sequence MAP decoder was implemented via a modified Viterbi algorithm. The sources were generated according to a bivariate Gaussian distribution with a correlation coefficient modeled via a two-state Markov process causing change in the joint distribution over time and creating temporal memory in the joint source symbols. Under two-level scalar quantization, we established necessary and sufficient conditions under which

a simple instantaneous symbol-by-symbol joint decoder can replace the joint sequence MAP decoder without loss of optimality. Finally, numerical results validated our theoretical results and demonstrated that the proposed system can judiciously make use of the sources' correlation, temporal memory and statistics, as well as of the channel's temporal memory and soft-decision information to provide a robust SDR performance.

Future work includes investigating how to efficiently reduce the Viterbi MAP decoder's complexity, which grows exponentially with the NBNDQ noise memory M ; this can be pursued by a possible extension of the approach in [29]. Finding necessary and sufficient conditions under which the joint sequence MAP decoder becomes unnecessary is still an open problem for systems with channel noise memory order or scalar quantization rates greater than one. Systematically evaluating the system's modeling effectiveness under a joint sequence MAP decoder by fitting the MAC's NBNDQ sub-channels to the underlying MAC fading channel is also an interesting research direction.⁵ Studying this system for the regular (non-orthogonal) MAC with correlated fading, possibly using interference mitigation techniques such as in [41], is another worthwhile objective. Furthermore, generalizing this work from two to multiple users is of interest. Many emerging topics such as data survivability in distributed data storage can benefit from harnessing the correlation (or any other shared information) between users to jointly decode data transmitted to a common node. Moreover, identifying general conditions under which a simple instantaneous joint decoder is enough to optimally decode the messages, can help give guidelines on how to distribute the data and optimize the system.

APPENDIX A

PROOF OF LEMMA 1

When the underlying source $\{(V_i, V'_i)\}$ described in Section II-A is binary-quantized ($n = 1$), where each SQ sets its quantization threshold to zero, then due to the symmetry of the bivariate Gaussian density (1), the conditional distribution vectors $\pi_\phi \triangleq [P_{\text{HMM}}\{(X_i, X'_i) = (0, 0) \mid \Phi_i = \phi\}, P_{\text{HMM}}\{(X_i, X'_i) = (0, 1) \mid \Phi_i = \phi\}, P_{\text{HMM}}\{(X_i, X'_i) = (1, 0) \mid \Phi_i = \phi\}, P_{\text{HMM}}\{(X_i, X'_i) =$

⁵Some preliminary modeling results are available in [36, Section 3.4.2].

$(1, 1) \mid \Phi_i = \phi\} \Big] , \phi \in \{\phi_0, \phi_1\}$, have identical first and last components and identical second and third components and admit the following form

$$\pi_{\phi_0} = [a', b', b', a'] \quad \text{and} \quad \pi_{\phi_1} = [c', d', d', c'] \quad (18)$$

where a', b', c' and d' are as given in (6). The hidden Markov model for $\{(X_i, X'_i)\}$ is depicted in Fig. 3. We approximate it with a first-order Markov source of identical second-order statistics.

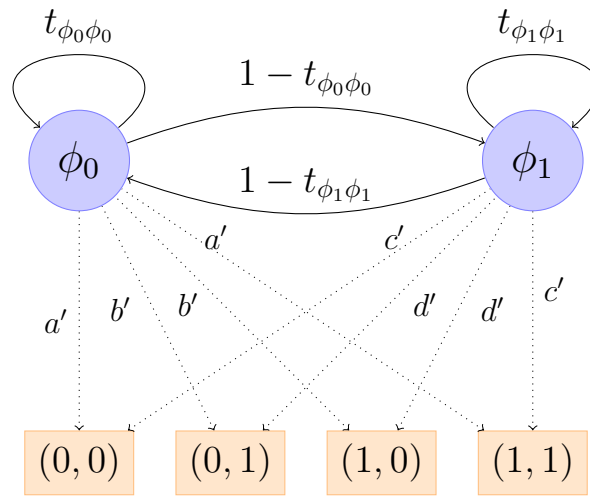


Fig. 3: HMM diagram: the hidden transition probabilities and emission probabilities are given by the corresponding edges.

Let

$$\Omega_{jk} \triangleq [P_{jk-00}, P_{jk-01}, P_{jk-10}, P_{jk-11}]$$

denote the rows of the Markov source's transition matrix T , $j, k \in \{0, 1\}$. Due to the underlying HMM, each component of Ω_{jk} satisfies

$$\begin{aligned} P_{jk-lm} &= P_{\text{HMM}} \{(X_i, X'_i) = (l, m) \mid \Phi_i = \phi_0\} P_{\text{HMM}} \{\Phi_i = \phi_0 \mid (X_{i-1}, X'_{i-1}) = (j, k)\} \\ &+ P_{\text{HMM}} \{(X_i, X'_i) = (l, m) \mid \Phi_i = \phi_1\} P_{\text{HMM}} \{\Phi_i = \phi_1 \mid (X_{i-1}, X'_{i-1}) = (j, k)\} \end{aligned} \quad (19)$$

where $l, m \in \{0, 1\}$. Now we can express $P_{\text{HMM}}\{\Phi_i = \phi_0 | (X_{i-1}, X'_{i-1}) = (0, 0)\}$ as follows

$$\begin{aligned}
P_{\text{HMM}}\{\Phi_i = \phi_0 | (X_{i-1}, X'_{i-1}) = (0, 0)\} \\
&= P_{\text{HMM}}\{\Phi_i = \phi_0 | \Phi_{i-1} = \phi_0\}P_{\text{HMM}}\{\Phi_{i-1} = \phi_0 | (X_{i-1}, X'_{i-1}) = (0, 0)\} \\
&\quad + P_{\text{HMM}}\{\Phi_i = \phi_0 | \Phi_{i-1} = \phi_1\}P_{\text{HMM}}\{\Phi_{i-1} = \phi_1 | (X_{i-1}, X'_{i-1}) = (0, 0)\} \\
&= t_{\phi_0\phi_0} \times \frac{P_{\text{HMM}}\{(X_{i-1}, X'_{i-1}) = (0, 0) | \Phi_{i-1} = \phi_0\} \Pr\{\Phi_{i-1} = \phi_0\}}{P_{\text{HMM}}\{(X_{i-1}, X'_{i-1}) = (0, 0)\}} \\
&\quad + (1 - t_{\phi_1\phi_1}) \times \frac{P_{\text{HMM}}\{(X_{i-1}, X'_{i-1}) = (0, 0) | \Phi_{i-1} = \phi_1\} \Pr\{\Phi_{i-1} = \phi_1\}}{P_{\text{HMM}}\{(X_{i-1}, X'_{i-1}) = (0, 0)\}} \\
&= \frac{t_{\phi_0\phi_0} \times a' \times P_{\phi_0} + (1 - t_{\phi_1\phi_1}) \times c' \times (1 - P_{\phi_0})}{a' \times P_{\phi_0} + c' \times (1 - P_{\phi_0})}, \tag{20}
\end{aligned}$$

where $P_{\phi_0} \triangleq \Pr\{\Phi_i = \phi_0\} = 1 - \Pr\{\Phi_i = \phi_1\} = \frac{1 - t_{\phi_1\phi_1}}{2 - (t_{\phi_0\phi_0} + t_{\phi_1\phi_1})}$ is the stationary distribution of the Markov process $\{\Phi_i\}_{i=1}^{\infty}$. Similarly, it can be shown that

$$P_{\text{HMM}}\{\Phi_i = \phi_1 | (X_{i-1}, X'_{i-1}) = (0, 0)\} = \frac{(1 - t_{\phi_0\phi_0})a'P_{\phi_0} + t_{\phi_1\phi_1}c'(1 - P_{\phi_0})}{a'P_{\phi_0} + c'(1 - P_{\phi_0})}. \tag{21}$$

Finally, using (18)-(21), we obtain the following expressions for the rows of T

$$\begin{aligned}
\Omega_{00} = \Omega_{11} &= \frac{\pi_{\phi_0}[a't_{\phi_0\phi_0}P_{\phi_0} + c'(1 - t_{\phi_1\phi_1})(1 - P_{\phi_0})] + \pi_{\phi_1}[a'(1 - t_{\phi_0\phi_0})P_{\phi_0} + c't_{\phi_1\phi_1}(1 - P_{\phi_0})]}{a'P_{\phi_0} + c'(1 - P_{\phi_0})} \\
\Omega_{01} = \Omega_{10} &= \frac{\pi_{\phi_0}[b't_{\phi_0\phi_0}P_{\phi_0} + d'(1 - t_{\phi_1\phi_1})(1 - P_{\phi_0})] + \pi_{\phi_1}[b'(1 - t_{\phi_0\phi_0})P_{\phi_0} + d't_{\phi_1\phi_1}(1 - P_{\phi_0})]}{b'P_{\phi_0} + d'(1 - P_{\phi_0})}
\end{aligned}$$

where the above is written in scalar (component-wise) multiplication form; this completes the proof of Lemma 1.

APPENDIX B

PROOF⁶ OF THEOREM 1

For the pair of instantaneous mappings (θ^*, θ'^*) to be an optimal joint MAP sequence decoder in the sense of minimizing the joint sequence error probability (i.e., to be equivalent to the joint

⁶Given its length, we herein present an abridged proof; see [36, Appendix B] for the fully detailed proof.

sequence MAP decoder), it is necessary and sufficient that for all input sequences $(x, x')^N \in (\mathcal{X} \times \mathcal{X}')^N$ and output sequences $(y, y')^N \in (\mathcal{Y} \times \mathcal{Y}')^N$, where $\mathcal{X} = \mathcal{X}' = \{0, 1\}$ and $\mathcal{Y} = \{0, 1, \dots, 2^q - 1\}$ and $\mathcal{Y}' = \{0, 1, \dots, 2^{q'} - 1\}$, the following holds

$$\gamma \triangleq \frac{\Pr \{(X, X')^N = (\tilde{y}, \tilde{y}')^N | (Y, Y')^N = (y, y')^N\}}{\Pr \{(X, X')^N = (x, x')^N | (Y, Y')^N = (y, y')^N\}} \geq 1 \quad (22)$$

where $(\tilde{y}, \tilde{y}')^N \triangleq (\theta^*(y), \theta'^*(y'))^N$ represents the sequence of simultaneously decoded pairs (i.e., $\tilde{y}_i = \theta^*(y_i)$ and $\tilde{y}'_i = \theta'^*(y'_i)$, $i = 1, 2, \dots, N$).

A. Preliminaries

Note that γ can be written as

$$\gamma = \frac{\Pr \{(Y, Y')^N = (y, y')^N | (X, X')^N = (\tilde{y}, \tilde{y}')^N\} \Pr \{(X, X')^N = (\tilde{y}, \tilde{y}')^N\}}{\Pr \{(Y, Y')^N = (y, y')^N | (X, X')^N = (x, x')^N\} \Pr \{(X, X')^N = (x, x')^N\}}. \quad (23)$$

Since the two sub-channels of the MAC are orthogonal and the input sequences are independent of the noise processes, we have

$$\begin{aligned} \gamma &= \frac{\Pr \{Y_1^N = y_1^N | X_1^N = \tilde{y}_1^N\} \Pr \{Y_1'^N = y_1'^N | X_1'^N = \tilde{y}_1'^N\} \Pr \{(X, X')^N = (\tilde{y}, \tilde{y}')^N\}}{\Pr \{Y_1^N = y_1^N | X_1^N = x_1^N\} \Pr \{Y_1'^N = y_1'^N | X_1'^N = x_1'^N\} \Pr \{(X, X')^N = (x, x')^N\}} \\ &= \frac{\Pr \{Z_1^N = a_1^N\} \Pr \{Z_1'^N = a_1'^N\} \Pr \{(X, X')^N = (\tilde{y}, \tilde{y}')^N\}}{\Pr \{Z_1^N = z_1^N\} \Pr \{Z_1'^N = z_1'^N\} \Pr \{(X, X')^N = (x, x')^N\}} \\ &= \frac{\Pr \{Z_1 = a_1\} \Pr \{Z_1' = a_1'\} P(\tilde{y}_1, \tilde{y}_1') \prod_{k=2}^N \frac{Q(a_k | a_{k-1}) Q'(a_k' | a_{k-1}') P((\tilde{y}_k, \tilde{y}_k') | (\tilde{y}_{k-1}, \tilde{y}_{k-1}'))}{\Pr \{Z_1 = z_1\} \Pr \{Z_1' = z_1'\} P(x_1, x_1') \prod_{k=2}^N \frac{Q(z_k | z_{k-1}) Q'(z_k' | z_{k-1}') P((x_k, x_k') | (x_{k-1}, x_{k-1}'))}}{\prod_{k=2}^N \frac{Q(a_k | a_{k-1}) Q'(a_k' | a_{k-1}') P((\tilde{y}_k, \tilde{y}_k') | (\tilde{y}_{k-1}, \tilde{y}_{k-1}'))}{Q(z_k | z_{k-1}) Q'(z_k' | z_{k-1}') P((x_k, x_k') | (x_{k-1}, x_{k-1}'))}}, \quad (24) \end{aligned}$$

where, for $i = 1, 2, \dots, N$, $z_i \triangleq \frac{y_i - (2^q - 1)x_i}{(-1)^{x_i}}$ and $a_i \triangleq \frac{y_i - (2^q - 1)\tilde{y}_i}{(-1)^{\tilde{y}_i}}$; and $z'_i \triangleq \frac{y'_i - (2^{q'} - 1)x'_i}{(-1)^{x'_i}}$ and $a'_i \triangleq \frac{y'_i - (2^{q'} - 1)\tilde{y}'_i}{(-1)^{\tilde{y}'_i}}$. Since θ and θ^* are in the form of (8), we have $a_i \leq 2^{q-1} - 1$ and $a'_i \leq 2^{q'-1} - 1$, for any $i \in \{1, 2, \dots, N\}$. The last two equations in (24) follow from the assumptions that $x_1 = \tilde{y}_1$ and $x'_1 = \tilde{y}'_1$ in Theorem 1 which result in $z_1 = a_1$ and $z'_1 = a'_1$, respectively, and the fact that for an NBNDC-QB sub-channel with $M = 1$, the noise process is a homogeneous first-order Markov process with $\Pr\{Z_k = z_k\} = \rho_{z_k}$, and $Q(z_k | z_{k-1}) = [\epsilon \delta_{z_k, z_{k-1}} + (1 - \epsilon) \rho_{z_k}]$,

$z_k, z_{k-1} \in \mathcal{Y}$; $\delta_{z_k, z_{k-1}} = 1$ if $z_k = z_{k-1}$ and $\delta_{z_k, z_{k-1}} = 0$ otherwise.

Next, we review some properties regarding the NBNDC-QB sub-channels. Considering the first sub-channel, the following hold [16, Appendix C]. For any $k \in \{2, \dots, N\}$,

- We have

$$z_k = \begin{cases} a_k, & \text{if } z_k \leq 2^{q-1} - 1 \\ 2^q - 1 - a_k, & \text{if otherwise.} \end{cases} \quad (25)$$

- If $x_k = \tilde{y}_k$ and $x_{k-1} = \tilde{y}_{k-1}$,

$$\frac{Q(a_k|a_{k-1}) Q(a_k|a_{k-1})}{Q(z_k|z_{k-1}) Q(a_k|a_{k-1})} = 1. \quad (26)$$

- If $x_k = \tilde{y}_k$ and $x_{k-1} \neq \tilde{y}_{k-1}$,

$$\min \frac{Q(a_k|a_{k-1})}{Q(z_k|z_{k-1})} = \min \frac{Q(a_k|a_{k-1})}{Q(a_k|2^q - 1 - a_{k-1})} = 1 \quad (27)$$

where equality holds if and only if $a_k \neq a_{k-1}$.

- If $x_k \neq \tilde{y}_k$ and $x_{k-1} = \tilde{y}_{k-1}$,

$$\min \frac{Q(a_k|a_{k-1})}{Q(z_k|z_{k-1})} = \min \frac{Q(a_k|a_{k-1})}{Q(2^q - 1 - a_k|a_{k-1})} = \frac{\rho_{2^q-1-1}}{\rho_{2^q-1}} \quad (28)$$

where equality holds if $z_k = 2^{q-1}$ and $a_k \neq a_{k-1}$.

- If $x_k \neq \tilde{y}_k$ and $x_{k-1} \neq \tilde{y}_{k-1}$,

$$\min \frac{Q(a_k|a_{k-1})}{Q(z_k|z_{k-1})} = \min \frac{Q(a_k|a_{k-1})}{Q(2^q - 1 - a_k|2^q - 1 - a_{k-1})} = \frac{\epsilon + (1 - \epsilon)\rho_{2^q-1-1}}{\epsilon + (1 - \epsilon)\rho_{2^q-1}} \quad (29)$$

where equality holds if $z_k = z_{k-1} = 2^{q-1}$.

The above results also apply for the second sub-channel using its corresponding parameters.

We next partition the index set $\mathcal{K} = \{2, 3, \dots, N\}$ as $\mathcal{K} = \bigcup_{i=0}^{15} \mathcal{A}_i$, where

$$\mathcal{A}_i \triangleq \{k \in \mathcal{K} : x_k \oplus \tilde{y}_k = i_3, x'_k \oplus \tilde{y}'_k = i_2, x_{k-1} \oplus \tilde{y}_{k-1} = i_1, x'_{k-1} \oplus \tilde{y}'_{k-1} = i_0\}, \quad (30)$$

the binary 4-tuple $(i_3 i_2 i_1 i_0)$ is the binary representation of i and \oplus denotes addition in modulo-2.

Using the \mathcal{A}_i sets, we can rewrite γ as

$$\gamma = \prod_{i=0}^{15} \gamma_i = \prod_{i=0}^{15} \prod_{k \in \mathcal{A}_i} \gamma_{\mathcal{A}_i}, \quad (31)$$

where $\gamma_i = \prod_{k \in \mathcal{A}_i} \gamma_{\mathcal{A}_i}$ and

$$\gamma_{\mathcal{A}_i} \triangleq \frac{Q(a_k|a_{k-1})Q'(a'_k|a'_{k-1})P((\tilde{y}_k, \tilde{y}'_k)|(\tilde{y}_{k-1}, \tilde{y}'_{k-1}))}{Q(z_k|z_{k-1})Q'(z'_k|z'_{k-1})P((x_k, x'_k)|(x_{k-1}, x'_{k-1}))}. \quad (32)$$

In order to achieve a sufficient/necessary condition for optimal detection, we need to find a lower bound for γ using the Markov source transition matrix T and the results in (26)-(29). So a comparison between the γ_i 's, $i = 0, \dots, 15$ is required. For the cases $\mathcal{A}_0, \mathcal{A}_3, \mathcal{A}_{12}$, and \mathcal{A}_{15} , we will have that each of $\gamma_0, \gamma_3, \gamma_{12}$, and γ_{15} are greater than or equal to one; so we evaluate the other cases by comparing their $\gamma_{\mathcal{A}_i}$'s. It can be shown that [36, Appendix B.1]

$$\begin{aligned} \gamma_{\mathcal{A}_1} \leq \gamma_{\mathcal{A}_{13}} \quad \text{and} \quad \gamma_{\mathcal{A}_7} < \gamma_{\mathcal{A}_5} \leq \gamma_{\mathcal{A}_6} \quad \text{and} \quad \gamma_{\mathcal{A}_7} \leq \gamma_{\mathcal{A}_4} < \gamma_{\mathcal{A}_6} \\ \gamma_{\mathcal{A}_2} \leq \gamma_{\mathcal{A}_{14}} \quad \text{and} \quad \gamma_{\mathcal{A}_{11}} \leq \gamma_{\mathcal{A}_8} < \gamma_{\mathcal{A}_9} \quad \text{and} \quad \gamma_{\mathcal{A}_{11}} < \gamma_{\mathcal{A}_{10}} \leq \gamma_{\mathcal{A}_9}. \end{aligned} \quad (33)$$

Further comparison requires more knowledge about sub-channel parameters (SNR, q, ϵ) and (SNR', q', ϵ').

For any pair of input and output sequences $\{(X_i, Y_i)\}_{i=1}^{\infty}$, we define a sequence of states $\{\mathcal{S}_i\}_{i=2}^{\infty}$, where $\mathcal{S}_i = \mathcal{A}_j, j \in \{0, \dots, 15\}$, if $i \in \mathcal{A}_j$ by definition of the partitions. Since each state \mathcal{S}_i depends on the (x_i, y_i) and (x'_i, y'_i) as well as (x_{i-1}, y_{i-1}) and (x'_{i-1}, y'_{i-1}) , any state can only be followed by certain states which are specified in [36, Table B.1].

B. Necessary Conditions

Considering the results in the previous section and writing the necessary condition in (11) as

$$\min \{\gamma_{\mathcal{A}_4}, \gamma_{\mathcal{A}_8}\} = \min \left\{ \frac{\rho_{2^{q-1}-1}}{\rho_{2^q-1}}, \frac{\rho'_{2^{q'-1}-1}}{\rho'_{2^{q'}-1}} \right\} \times \min \left\{ \frac{a}{b}, \frac{b}{a}, \frac{c}{d}, \frac{d}{c} \right\} < 1, \quad (34)$$

it can be shown that if the condition does not hold, a pair of input and output sequences which results in $\gamma < 1$ can be found, meaning that the pair of mappings (θ, θ') given in (8) is not optimal joint sequence MAP detector [36, Appendix B.2]. As an illustration of the method used,

we herein present the proof for the case when N is large enough: if the necessary condition (12) does not hold, then

$$\min \left\{ A \min \left\{ \frac{a}{d}, \frac{d}{a} \right\}, \min \left\{ \frac{\rho_{2^{q-1}-1}}{\rho_{2^q-1}}, \frac{\rho'_{2^{q'-1}-1}}{\rho'_{2^{q'}-1}} \right\} \times \min \left\{ \frac{a^2}{bc}, \frac{bc}{a^2}, \frac{bc}{d^2}, \frac{d^2}{bc} \right\} \right\} < 1, \quad (35)$$

where

$$A = \min \left\{ \frac{\epsilon' + (1 - \epsilon')\rho'_{2^{q'-1}-1}}{\epsilon' + (1 - \epsilon')\rho'_{2^{q'}-1}}, \frac{\epsilon + (1 - \epsilon)\rho_{2^{q-1}-1}}{\epsilon + (1 - \epsilon)\rho_{2^q-1}} \right\}.$$

There are two possible cases:

- 1) Assume that $A \times \min \left\{ \frac{a}{d}, \frac{d}{a} \right\} < 1$. Without loss of generality, set $A = \frac{\epsilon + (1 - \epsilon)\rho_{2^{q-1}-1}}{\epsilon + (1 - \epsilon)\rho_{2^q-1}}$.

If $\min \left\{ \frac{a}{d}, \frac{d}{a} \right\} = \frac{a}{d}$, the input and output sequences $(x, x')^N = ((0, 1), (0, 1), \dots, (0, 1))$ and $(y, y')^N = ((0, 1), (2^{q-1}, 1), (2^{q-1}, 1), \dots, (2^{q-1}, 1))$ result in

$$\gamma = \frac{\rho_{2^{q-1}-1}}{\rho_{2^q-1}} \times \frac{a}{d} \times \left(\frac{\epsilon + (1 - \epsilon)\rho_{2^{q-1}-1}}{\epsilon + (1 - \epsilon)\rho_{2^q-1}} \times \frac{a}{d} \right)^{N-1}$$

which tends to zero as $N \rightarrow \infty$.

If $\min \left\{ \frac{a}{d}, \frac{d}{a} \right\} = \frac{d}{a}$, the input and output sequences $(x, x')^N = ((0, 0), (0, 0), \dots, (0, 0))$ and $(y, y')^N = ((0, 0), (2^{q-1}, 0), (2^{q-1}, 0), \dots, (2^{q-1}, 0))$ result in

$$\gamma = \frac{\rho_{2^{q-1}-1}}{\rho_{2^q-1}} \times \frac{d}{a} \times \left(\frac{\epsilon + (1 - \epsilon)\rho_{2^{q-1}-1}}{\epsilon + (1 - \epsilon)\rho_{2^q-1}} \times \frac{d}{a} \right)^{N-1}$$

which tends to zero as $N \rightarrow \infty$.

Similarly, if $A = \frac{\epsilon' + (1 - \epsilon')\rho'_{2^{q'-1}-1}}{\epsilon' + (1 - \epsilon')\rho'_{2^{q'}-1}}$, switching x with x' and y with y' in the above input and output sequence examples will result in γ becoming arbitrarily small for a large enough N .

- 2) Assume that $\min \left\{ \frac{\rho_{2^{q-1}-1}}{\rho_{2^q-1}}, \frac{\rho'_{2^{q'-1}-1}}{\rho'_{2^{q'}-1}} \right\} \times \min \left\{ \frac{a^2}{bc}, \frac{bc}{a^2}, \frac{bc}{d^2}, \frac{d^2}{bc} \right\} < 1$.

It can be verified that the input and output sequences given as examples in the proof of the necessary condition (11) for general N will result in the $\gamma < 1$ for a large enough N .

As an example, if $\min \left\{ \frac{\rho_{2^{q-1}-1}}{\rho_{2^q-1}}, \frac{\rho'_{2^{q'-1}-1}}{\rho'_{2^{q'}-1}} \right\} \times \min \left\{ \frac{a^2}{bc}, \frac{bc}{a^2}, \frac{bc}{d^2}, \frac{d^2}{bc} \right\} = \frac{\rho'_{2^{q'-1}-1}}{\rho'_{2^{q'}-1}} \frac{bc}{d^2}$, the input and output sequences $(x, x')^N = ((0, 1), (0, 1), \dots, (0, 1))$ and $(y, y')^N = ((0, 1), (0, 2^{q-1} -$

1), (0, 1), (0, $2^{q-1} - 1$), ...) result in

$$\gamma = \frac{\rho'_{2^{q'-1}-1}}{\rho'_{2^{q'-1}}} \frac{c}{d} \times \frac{b}{d} \times \frac{\rho'_{2^{q'-1}-1}}{\rho'_{2^{q'-1}}} \frac{c}{d} \times \frac{b}{d} \times \dots \leq \frac{\rho'_{2^{q'-1}-1}}{\rho'_{2^{q'-1}}} \left\{ \frac{\rho'_{2^{q'-1}-1}}{\rho'_{2^{q'-1}}} \frac{bc}{d^2} \right\}^{\lfloor \frac{N-1}{2} \rfloor}$$

which tends to zero as $N \rightarrow \infty$. Thus, there exists N large enough for which $\gamma < 1$.

C. Sufficient Condition

We show that γ computed via (24) for any input and output sequences $\{(x_i, x'_i)\}_{i=1}^N$ and $\{(y_i, y'_i)\}_{i=1}^N$ with $N \geq 2$ is greater than or equal to one under the condition (9).

First, if (9) holds, we will have

$$\min \{\gamma_{\mathcal{A}_7}, \gamma_{\mathcal{A}_{11}}\} \times \gamma_{\mathcal{A}_1} \geq 1. \quad (36)$$

This inequality along with those in (33) results in $\gamma_{\mathcal{A}_i} \geq 1$ for all $i \in \{0, 3, 4, \dots, 15\}$, which implies that only $\gamma_{\mathcal{A}_1}$ and $\gamma_{\mathcal{A}_2}$ are less than one.

Now, assume that $\{\mathcal{S}_i\}_{i=2}^N$ is the state sequence assigned to an arbitrary input and output sequences $\{(x_i, x'_i)\}_{i=1}^N$ and $\{(y_i, y'_i)\}_{i=1}^N$. We can write the following lower bound for γ

$$\gamma \geq \prod_{i=1}^N \gamma_{\mathcal{S}_i}, \quad (37)$$

where $\gamma_{\mathcal{S}_i} \in \{\gamma_{\mathcal{A}_1}, \dots, \gamma_{\mathcal{A}_{15}}\}$, $i = 2, 3, \dots, N$. In fact,

$$\frac{Q(a_i|a_{i-1})Q'(a'_i|a'_{i-1})P((\tilde{y}_i, \tilde{y}'_i)|(\tilde{y}_{i-1}, \tilde{y}'_{i-1}))}{Q(z_i|z_{i-1})Q'(z'_i|z'_{i-1})P((x_i, x'_i)|(x_{i-1}, x'_{i-1}))} \geq \gamma_{\mathcal{S}_i}.$$

Note that the proposed lower bound only depends on the corresponding state sequence and not on the exact values of input and output sequences.

Finally, the proof is completed via strong induction and using (36) and the previous facts; see [36, Appendix B.3]. ■

REFERENCES

- [1] S. Beheshti, F. Alajaji, and T. Linder, "MAP decoding of correlated sources over soft-decision orthogonal multiple access fading channels with memory," in *Proc. IEEE Veh. Technol. Conf. (VTC Fall)*, Sep. 2014, pp. 1–5.

- [2] M. Liu, N. Patwari, and A. Terzis, "Special issue on sensor network applications," *Proc. IEEE*, vol. 98, no. 11, Nov. 2010.
- [3] W. Dargie and C. Poellabauer, *Fundamentals of Wireless Sensor Networks: Theory and Practice*, Wiley, 2010.
- [4] K. Sohraby, D. Minoli, and T. Znati, *Wireless Sensor Networks: Technology, Protocols, and Applications*, Wiley, 2007.
- [5] J. L. Massey, "Joint source and channel coding," in *Communications and Random Process Theory*, J. K. Skwirzynski, ed., The Netherlands: Sijthoff and Nordhoff, pp. 279–293, 1978.
- [6] H. Kumazawa, M. Kasahara, and T. Namekawa, "A construction of vector quantizers for noisy channels," *Electronics and Communications in Japan (Part I: Communications)*, vol. 67, no. 4, pp. 39–47, 1984.
- [7] N. Farvardin and V. Vaishampayan, "On the performance and complexity of channel-optimized vector quantizers," *IEEE Trans. Inform. Theory*, vol. 37, no. 1, pp. 155–160, Jan. 1991.
- [8] J. Hagenauer, "Source-controlled channel decoding," *IEEE Trans. Commun.*, vol. 43, pp. 2449–2457, Sep. 1995.
- [9] N. Phamdo, F. Alajaji, and N. Farvardin, "Quantization of memoryless and Gauss-Markov sources over binary Markov channels," *IEEE Trans. Commun.*, vol. 45, no. 6, pp. 668–675, Jun. 1997.
- [10] A. Goldsmith and M. Effros, "Joint design of fixed-rate source codes and multiresolution channel codes," *IEEE Trans. Commun.*, vol. 46, no. 10, pp. 1301–1312, Oct. 1998.
- [11] J. Lim and D. Neuhoff, "Joint and tandem source-channel coding with complexity and delay constraints," *IEEE Trans. Commun.*, vol. 51, no. 5, pp. 757–766, May 2003.
- [12] Y. Zhong, F. Alajaji and L. L. Campbell, "On the joint source-channel coding error exponent for discrete memoryless systems," *IEEE Trans. Inf. Theory*, vol. 52, no. 4, pp. 1450–1468, Apr. 2006.
- [13] N. Görtz, *Joint Source-Channel Coding of Discrete-Time Signals with Continuous Amplitudes*, Imperial College Press, London, UK, 2007.
- [14] P. Duhamel and M. Kieffer, *Joint Source-Channel Decoding: A Cross-Layer Perspective with Applications in Video Broadcasting over Mobile and Wireless Networks*, Academic Press, 2009.
- [15] J. Kron, F. Alajaji and M. Skoglund, "Low-delay joint source-channel mappings for the Gaussian MAC," *IEEE Commun. Letters*, vol. 18, no. 2, pp. 249–252, Feb. 2014.
- [16] S. Shahidi, F. Alajaji, and T. Linder, "MAP detection and robust lossy coding over soft-decision correlated fading channels," *IEEE Trans. Veh. Technol.*, vol. 62, no. 7, pp. 3175–3187, Sep. 2013.
- [17] C. Pimentel, F. Alajaji, and P. Melo, "A discrete queue-based model for capturing memory and soft-decision information in correlated fading channels," *IEEE Trans. Commun.*, vol. 60, no. 6, pp. 1702–1711, Jun. 2012.
- [18] R. L. Dobrushin and M. S. Pinsker, "Memory increases transmission capacity," *Problemy Peredachi Informatsii*, vol. 5, no. 1, pp. 94–95, 1969.
- [19] L. Zhong, F. Alajaji, and G. Takahara, "A binary communication channel with memory based on a finite queue," *IEEE Trans. Inf. Theory*, vol. 53, pp. 2815–2840, Aug. 2007.
- [20] J. Singh, O. Dabeer, and U. Madhow, "On the limits of communication with low-precision analog-to-digital conversion at the receiver," *IEEE Trans. Commun.*, vol. 57, no. 12, pp. 3629–3639, Dec. 2009.
- [21] J. Devore, "A note on the observation of a Markov source through a noisy channel," *IEEE Trans. Inf. Theory*, vol. 20, no. 6, pp. 762–764, Nov. 1974.

- [22] N. Phamdo and N. Farvardin, "Optimal detection of discrete Markov sources over discrete memoryless channels – applications to combined source-channel coding," *IEEE Trans. Inf. Theory*, vol. 40, no. 1, pp. 186–193, Jan. 1994.
- [23] F. Alajaji, N. Phamdo, N. Farvardin, and T. E. Fuja, "Detection of binary Markov sources over channels with additive Markov noise," *IEEE Trans. Inf. Theory*, vol. 42, no. 1, pp. 230–239, Jan. 1996.
- [24] D. Miller and M. Park, "A sequence-based approximate MMSE decoder for source coding over noisy channels using discrete hidden Markov models," *IEEE Trans. Commun.*, vol. 46, no. 2, pp. 222–231, Feb. 1998.
- [25] M. Skoglund, "Soft decoding for vector quantization over noisy channels with memory," *IEEE Trans. Inf. Theory*, vol. 45, no. 4, pp. 1293–1307, May 1999.
- [26] T. Fingscheidt, T. Hindelang, R. V. Cox and N. Seshadri, "Joint source-channel (de)coding for mobile communications," *IEEE Trans. Commun.*, vol. 50, pp. 200–212, Feb. 2002.
- [27] K. P. Subbalakshmi and J. Vaisey, "On the joint source-channel decoding of variable-length encoded sources: the additive-Markov case," *IEEE Trans. Commun.*, vol. 51, no. 9, pp. 1420–1425, Sep. 2003.
- [28] E. Ordentlich and T. Weissman, "On the optimality of symbol-by-symbol filtering and denoising," *IEEE Trans. Inf. Theory*, vol. 52, no. 1, pp. 19–40, Jan. 2006.
- [29] S. Dumitrescu, "Fast joint source-channel decoding of convolutional coded Markov sequences with Monge property," *IEEE Trans. Commun.*, vol. 58, no. 1, pp. 128–135, Jan. 2010.
- [30] L. Zhong, F. Alajaji, and G. Takahara, "A model for correlated Rician fading channels based on a finite queue," *IEEE Trans. Veh. Technol.*, vol. 57, no. 1, pp. 79–89, Jan. 2008.
- [31] P. Melo, C. Pimentel and F. Alajaji, "LDPC decoding over non-binary queue-based burst noise channels," *IEEE Trans. Veh. Technol.*, vol. 65, no. 1, pp. 452–457, Jan. 2016.
- [32] R. H. Clarke, "A statistical theory of mobile radio reception," *Bell Syst. Tech. J.*, vol. 47, no. 6, pp. 957–1000, 1968.
- [33] Y. Chen and C. Tellambura, "Infinite series representations of the trivariate and quadrivariate Rayleigh distribution and their applications," *IEEE Trans. Commun.*, vol. 53, no. 12, pp. 2092–2101, Dec. 2005.
- [34] G. Taricco, "On the capacity of the binary input Gaussian and Rayleigh fading channels," *Eur. Trans. Telecomm.*, vol. 7, pp. 201–208, Mar.-Apr. 1996.
- [35] C. Pimentel and F. Alajaji, "Packet-based modeling of Reed-Solomon block coded correlated fading channels via a Markov finite queue model," *IEEE Trans. Veh. Technol.*, vol. 58, no. 7, pp. 3124–3136, Sep. 2009.
- [36] S. Beheshti, *MAP Decoding of Correlated Sources over Soft-Decision Orthogonal Multiple Access Fading Channels with Memory*, M.Sc. Thesis, Queen's University, 2014. [Online]. Available: <http://hdl.handle.net/1974/12492>
- [37] S. Lloyd, "Least squares quantization in PCM," *IEEE Trans. Inf. Theory*, vol. 28, no. 2, pp. 129–137, Mar. 1982.
- [38] Y. Linde, A. Buzo, and R. Gray, "An algorithm for vector quantizer design," *IEEE Trans. Commun.*, vol. 28, no. 1, pp. 84–95, Jan. 1980.
- [39] J. Forney, G.D., "The Viterbi algorithm," *Proc. IEEE*, vol. 61, no. 3, pp. 268–278, Mar. 1973.
- [40] S. Shahidi, F. Alajaji, and T. Linder, "MAP decoding of quantized sources over soft-decision fading channels with memory," in *Proc. IEEE Int. Conf. Commun.*, 2012, pp. 2277–2282.
- [41] M. R. Bhatnagar and A. Hjørungnes, "Improved interference cancellation scheme for two-user detection of Alamouti code," *IEEE Trans. Signal Process.*, vol. 59, no. 8, pp. 4459–4465, Aug. 2010.

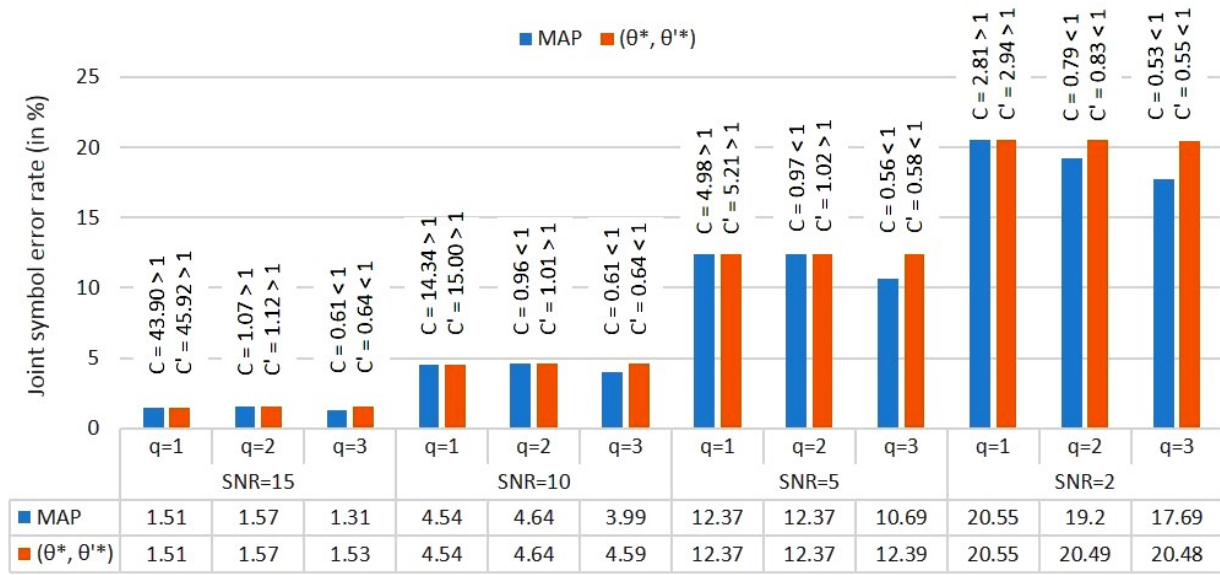


Fig. 4: Joint symbol error rate (in %) of joint MAP decoding and instantaneous joint decoding (θ^*, θ'^*) for two binary-quantized correlated Gaussian sources with Markovian correlation parameter. The channel model is a MAC with two orthogonal NBND-C-QB, with $M = \alpha = 1$, $Cor = Cor' = 0$ and identical parameters (SNR, q); $q = 1, 2, 3$. Source parameters are $\phi_{av} = 0.61$, $\phi_0 = -0.31$, $\phi_1 = 0.81$ and $(t_{\phi_0\phi_0}, t_{\phi_1\phi_1}) = (0.1, 0.8)$

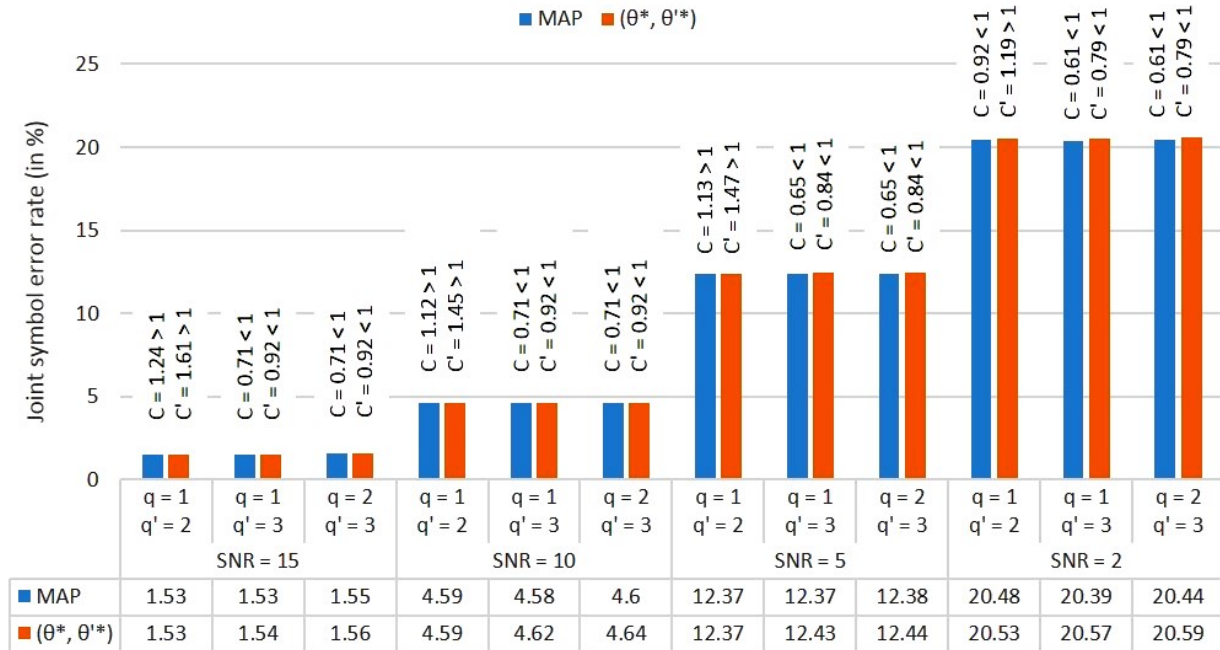


Fig. 5: Joint symbol error rate (in %) of joint MAP decoding and instantaneous joint decoding (θ^*, θ'^*) for two binary-quantized correlated Gaussian sources with Markovian correlation parameter. The channel model is a MAC with two orthogonal NBND-C-QB, with $M = \alpha = 1$, $Cor = Cor' = 0$, $q = 1, 2, 3$ and identical parameter SNR. Source parameters are $\phi_{av} = 0.25$, $\phi_0 = -0.31$, $\phi_1 = 0.81$ and $t_{\phi_0\phi_0} = t_{\phi_1\phi_1} = 0.2$

TABLE I: Joint symbol error rate (in % shown in **bold font**) of joint MAP decoding and instantaneous joint decoding (θ^*, θ'^*) for two binary-quantized correlated Gaussian sources with Markovian correlation parameter. The channel model is a MAC with two orthogonal NBNDQ-QB, with $M = \alpha = 1$, $Cor = Cor' = 0$ and $q = 1, 2, 3$. Source parameters: for $\phi_{av} = 0.25$, $\phi_0 = -0.31$, $\phi_1 = 0.81$ and $t_{\phi_0\phi_0} = t_{\phi_1\phi_1} = 0.2$; for $\phi_{av} = 0.61$, $\phi_0 = -0.31$, $\phi_1 = 0.81$ and $(t_{\phi_0\phi_0}, t_{\phi_1\phi_1}) = (0.1, 0.8)$.

Table I.(a): Two sub-channels with identical parameter SNR.

ϕ_{av}	(q, q')	(SNR, SNR') (dB)							
		(15,15)		(10,10)		(5,5)		(2,2)	
		MAP	(θ^*, θ'^*)	MAP	(θ^*, θ'^*)	MAP	(θ^*, θ'^*)	MAP	(θ^*, θ'^*)
0.25	(1,1)	$C = 51.00 > 1$		$C = 16.69 > 1$		$C = 5.80 > 1$		$C = 3.27 > 1$	
		$C' = 66.14 > 1$		$C' = 21.61 > 1$		$C' = 7.51 > 1$		$C' = 4.23 > 1$	
		1.52	1.52	4.56	4.56	12.49	12.49	20.59	20.59
	(2,2)	$C = 1.24 > 1$		$C = 1.12 > 1$		$C = 1.13 > 1$		$C = 0.92 < 1$	
		$C' = 1.61 > 1$		$C' = 1.45 > 1$		$C' = 1.47 > 1$		$C' = 1.19 > 1$	
		1.54	1.54	4.62	4.62	12.36	12.36	20.57	20.57
	(3,3)	$C = 0.71 < 1$		$C = 0.71 < 1$		$C = 0.65 < 1$		$C = 0.61 < 1$	
		$C' = 0.92 < 1$		$C' = 0.92 < 1$		$C' = 0.84 < 1$		$C' = 0.79 < 1$	
		1.51	1.54	4.54	4.61	12.23	12.44	20.34	20.58
0.61	(1,2)	$C = 1.07 > 1$		$C = 0.96 < 1$		$C = 0.97 < 1$		$C = 0.79 < 1$	
		$C' = 1.12 > 1$		$C' = 1.01 > 1$		$C' = 1.02 > 1$		$C' = 0.82 < 1$	
		1.55	1.55	4.60	4.60	12.41	12.41	19.72	20.55
	(1,3)	$C = 0.61 < 1$		$C = 0.61 < 1$		$C = 0.56 < 1$		$C = 0.53 < 1$	
		$C' = 0.64 < 1$		$C' = 0.64 < 1$		$C' = 0.58 < 1$		$C' = 0.55 < 1$	
		1.44	1.55	4.32	4.63	11.49	12.35	19.06	20.57
	(2,3)	$C = 0.61 < 1$		$C = 0.61 < 1$		$C = 0.56 < 1$		$C = 0.53 < 1$	
		$C' = 0.64 < 1$		$C' = 0.64 < 1$		$C' = 0.58 < 1$		$C' = 0.55 < 1$	
		1.44	1.56	4.33	4.61	11.59	12.44	18.37	20.53

Table I.(b): Two sub-channels with identical parameter q .

ϕ_{av}	(q, q')	(SNR, SNR') (dB)							
		(15,10)		(15,5)		(15,2)		(10,5)	
		MAP	(θ^*, θ'^*)	MAP	(θ^*, θ'^*)	MAP	(θ^*, θ'^*)	MAP	(θ^*, θ'^*)
0.25	(1,1)	$C = 16.70 > 1$		$C = 5.80 > 1$		$C = 3.27 > 1$		$C = 5.79 > 1$	
		$C' = 21.61 > 1$		$C' = 7.51 > 1$		$C' = 4.23 > 1$		$C' = 7.51 > 1$	
		3.10	3.10	7.16	7.16	11.45	11.45	8.59	8.59
	(2,2)	$C = 1.12 > 1$		$C = 1.13 > 1$		$C = 0.92 < 1$		$C = 1.12 > 1$	
		$C' = 1.45 > 1$		$C' = 1.47 > 1$		$C' = 1.19 > 1$		$C' = 1.45 > 1$	
		3.06	3.06	7.10	7.10	11.46	11.53	8.60	8.60
0.61	(1,1)	$C = 14.34 > 1$		$C = 4.98 > 1$		$C = 2.81 > 1$		$C = 4.98 > 1$	
		$C' = 15.00 > 1$		$C' = 5.21 > 1$		$C' = 2.94 > 1$		$C' = 5.21 > 1$	
		3.08	3.08	7.14	7.14	11.51	11.51	8.63	8.63
	(2,2)	$C = 0.96 < 1$		$C = 0.97 < 1$		$C = 0.79 < 1$		$C = 0.96 < 1$	
		$C' = 1.01 > 1$		$C' = 1.02 > 1$		$C' = 0.83 < 1$		$C' = 1.01 > 1$	
		3.11	3.11	7.10	7.12	10.76	11.59	8.62	8.62

TABLE II: Joint symbol error rate (in % shown in **bold font**) of joint MAP decoding and instantaneous joint decoding (θ^*, θ'^*) for two binary-quantized correlated Gaussian sources with Markovian correlation parameter. The channel model is a MAC with two orthogonal NBNDQ-QB, with $M = \alpha = 1$, $Cor = 5 \times 10^{-3}$, $Cor' = 0.5$ and $q = 1, 2, 3$. Source parameters: $\phi_{av} = 0$ with $\phi_0 = -0.5$, $\phi_1 = 0.5$ and $t_{\phi_0\phi_0} = t_{\phi_1\phi_1} = 0.2$.

Table II.(a): Two sub-channels with identical parameters (SNR, q).

ϕ_{av}	(q, q')	(SNR, SNR') (dB)							
		(15,15)		(10,10)		(5,5)		(2,2)	
		MAP	(θ^*, θ'^*)	MAP	(θ^*, θ'^*)	MAP	(θ^*, θ'^*)	MAP	(θ^*, θ'^*)
0.0	(1,1)	$C = 1.51 > 1$		$C = 1.48 > 1$		$C = 1.39 > 1$		$C = 1.31 > 1$	
		$C' = 112.39 > 1$		$C' = 36.72 > 1$		$C' = 12.75 > 1$		$C' = 7.19 > 1$	
		1.52	1.52	4.57	4.57	12.40	12.40	20.53	20.53
	(2,2)	$C = 0.78 < 1$		$C = 0.79 < 1$		$C = 0.84 < 1$		$C = 0.84 < 1$	
		$C' = 2.73 > 1$		$C' = 2.46 > 1$		$C' = 2.50 > 1$		$C' = 2.02 > 1$	
		1.54	1.54	4.64	4.64	12.46	12.46	20.42	20.42
	(3,3)	$C = 0.77 < 1$		$C = 0.77 < 1$		$C = 0.78 < 1$		$C = 0.79 < 1$	
		$C' = 1.57 > 1$		$C' = 1.57 > 1$		$C' = 1.43 > 1$		$C' = 1.35 > 1$	
		1.53	1.53	4.60	4.60	12.39	12.39	20.52	20.52

Table II.(b): Two sub-channels with identical parameter SNR.

ϕ_{av}	(q, q')	(SNR, SNR') (dB)							
		(15,15)		(10,10)		(5,5)		(2,2)	
		MAP	(θ^*, θ'^*)	MAP	(θ^*, θ'^*)	MAP	(θ^*, θ'^*)	MAP	(θ^*, θ'^*)
0.0	(1,2)	$C = 0.78 < 1$		$C = 0.79 < 1$		$C = 0.84 < 1$		$C = 0.85 < 1$	
		$C' = 2.74 > 1$		$C' = 2.47 > 1$		$C' = 2.50 > 1$		$C' = 2.02 > 1$	
		1.53	1.53	4.57	4.57	12.44	12.44	20.50	20.50
	(1,3)	$C = 0.77 < 1$		$C = 0.77 < 1$		$C = 0.78 < 1$		$C = 0.79 < 1$	
		$C' = 1.57 > 1$		$C' = 1.57 > 1$		$C' = 1.43 > 1$		$C' = 1.35 > 1$	
		1.52	1.52	4.57	4.57	12.52	12.52	20.48	20.48
	(2,3)	$C = 0.77 < 1$		$C = 0.77 < 1$		$C = 0.78 < 1$		$C = 0.79 < 1$	
		$C' = 1.57 > 1$		$C' = 1.57 > 1$		$C' = 1.43 > 1$		$C' = 1.35 > 1$	
		1.50	1.50	4.57	4.57	12.39	12.39	20.54	20.54
	(3,2)	$C = 0.78 < 1$		$C = 0.79 < 1$		$C = 0.84 < 1$		$C = 0.85 < 1$	
		$C' = 1.57 > 1$		$C' = 1.57 > 1$		$C' = 1.43 > 1$		$C' = 1.35 > 1$	
		1.58	1.58	4.62	4.62	12.46	12.46	20.52	20.52
	(3,1)	$C = 1.52 > 1$		$C = 1.48 > 1$		$C = 1.39 > 1$		$C = 1.31 > 1$	
		$C' = 2.74 > 1$		$C' = 2.47 > 1$		$C' = 2.50 > 1$		$C' = 2.02 > 1$	
		1.55	1.55	4.71	4.71	12.35	12.35	20.73	20.73
	(2,1)	$C = 1.52 > 1$		$C = 1.48 > 1$		$C = 1.39 > 1$		$C = 1.31 > 1$	
		$C' = 2.74 > 1$		$C' = 2.47 > 1$		$C' = 2.50 > 1$		$C' = 2.02 > 1$	
		1.55	1.55	4.71	4.71	12.35	12.35	20.73	20.73

TABLE III: SQ-MAC-MAP system: simulation SDR results (in dB) for two correlated Gaussian sources with Markovian correlation coefficient sent over the orthogonal MAC with memoryless NBND-C-QB sub-channels ($Cor = Cor' = 0.0$), moderately and highly correlated NBND-C-QB sub-channels ($Cor = Cor' = 0.5$ and $Cor = Cor' = 0.9$) with identical parameters (SNR, q) and $M = \alpha = 1$. Source parameters: for $\phi_{av} = 0.25$, $\phi_0 = -0.31$, $\phi_1 = 0.81$ and $t_{\phi_0\phi_0} = t_{\phi_1\phi_1} = 0.2$; for $\phi_{av} = 0.61$, $\phi_0 = -0.31$, $\phi_1 = 0.81$ and ($t_{\phi_0\phi_0}, t_{\phi_1\phi_1}$) = (0.1, 0.8).

ϕ_{av}	q	n	Fully interleaved (Cor=0)									Cor=0.5						Cor=0.9																																																																																																																																																																																																																																																															
			SNR (dB)			SNR (dB)			SNR (dB)			SNR (dB)			SNR (dB)			SNR (dB)			SNR (dB)																																																																																																																																																																																																																																																												
			15	10	5	2	5	10	15	10	5	2	5	10	15	10	5	2	5	10	15	10	5	2	5	10																																																																																																																																																																																																																																																							
0.25	1	1	4.17	3.75	2.77	1.94	1.94	4.17	3.74	2.77	1.93	1.93	4.17	3.72	2.77	1.94	2	1	8.14	6.47	3.81	2.06	2.06	8.21	6.63	4.10	2.42	2.42	8.41	7.05	4.94	3.50	3	1	11.06	7.75	3.92	2.00	2.00	11.13	7.83	4.11	2.09	2.09	11.68	9.06	5.72	3.75	1	1	4.16	3.73	2.79	1.94	1.94	4.17	3.76	2.81	1.97	1.97	4.23	3.94	3.09	2.32	2	2	8.23	6.65	4.06	2.48	2.48	8.41	7.01	4.53	2.88	2.88	8.88	8.05	6.28	4.83	3	1	4.17	3.76	2.83	1.97	1.97	4.18	3.77	2.87	2.04	2.04	4.25	3.97	3.22	2.47	2	2	8.27	6.69	4.15	2.47	2.47	8.47	7.13	4.75	3.09	3.09	8.95	8.25	6.72	5.43	3	1	11.45	8.34	4.65	2.63	2.63	11.92	9.11	5.44	3.27	3.27	13.46	11.66	8.60	6.59	0.61	1	1	4.16	3.75	2.78	1.94	1.94	4.15	3.75	2.79	1.93	1.93	4.19	3.73	2.74	1.78	2	2	8.12	6.48	3.79	1.69	1.69	8.23	6.64	4.16	2.51	2.51	8.67	7.72	5.88	4.52	3	1	10.94	7.74	3.87	1.86	1.86	11.06	7.89	4.37	2.44	2.44	12.42	10.18	6.97	5.13	1	1	4.17	3.76	2.81	2.20	2.20	4.24	3.91	3.09	2.31	2.31	4.35	4.16	3.69	3.02	2	2	8.39	7.03	4.67	3.04	3.04	8.63	7.49	5.23	3.55	3.55	9.06	8.60	7.38	6.05	3	1	11.78	8.91	5.19	3.19	3.19	12.44	9.65	5.97	3.74	3.74	13.80	12.24	9.46	7.45	1	1	4.22	3.88	3.07	2.28	2.28	4.27	3.97	3.24	2.48	2.48	4.35	4.24	3.89	3.33	2	2	8.46	7.15	4.82	3.10	3.10	8.69	7.61	5.49	3.87	3.87	9.13	8.82	7.85	6.81	3	1	11.94	9.09	5.48	3.36	3.36	12.54	10.06	6.42	4.23	4.23	13.98	12.83	10.39	8.63

TABLE IV: SQ with instantaneous decoder $(\theta^*, \theta^{*'})$ system: simulation SDR results (in dB) for two correlated Gaussian sources with Markovian correlation coefficient sent over the orthogonal MAC with memoryless NBNDQ-QB sub-channels ($Cor = Cor' = 0.0$), moderately and highly correlated NBNDQ-QB sub-channels ($Cor = Cor' = 0.5$ and $Cor = Cor' = 0.9$) with identical parameters (SNR, q) and $M = \alpha = 1$. Source parameters: for $\phi_{av} = 0.25$, $\phi_0 = -0.31$, $\phi_1 = 0.81$ and $t_{\phi_0\phi_0} = t_{\phi_1\phi_1} = 0.2$; for $\phi_{av} = 0.61$, $\phi_0 = -0.31$, $\phi_1 = 0.81$, $(t_{\phi_0\phi_0}, t_{\phi_1\phi_1}) = (0.1, 0.8)$.

ϕ_{av}	q	n	Fully interleaved (Cor=0)									Cor=0.5						Cor=0.9													
			SNR (dB)									SNR (dB)						SNR (dB)													
			15	10	5	2	2	5	10	15	4.17	15	10	5	2	2	5	10	15	4.17	15	10	5	2	2	5	10	15	4.17		
0.25	1	1	4.17	3.75	2.77	1.94	1.94	4.17	3.74	2.77	1.93	1.93	4.17	3.72	2.77	1.93	1.93	4.17	3.72	2.77	1.95	1.95	4.17	3.72	2.77	1.95	1.95	4.17	3.72	2.77	1.95
		2	8.14	6.47	3.85	2.11	2.11	8.21	6.63	4.10	2.41	2.41	8.31	6.76	4.30	2.71	2.71	8.31	6.76	4.30	2.71	2.71	8.31	6.76	4.30	2.71	2.71	8.31	6.76	4.30	2.71
		3	11.06	7.75	3.96	1.86	1.86	11.13	7.83	4.09	1.98	1.98	11.22	8.16	4.41	2.24	2.24	11.22	8.16	4.41	2.24	2.24	11.22	8.16	4.41	2.24	2.24	11.22	8.16	4.41	2.24
	2	1	4.16	3.73	2.79	1.94	1.94	4.17	3.74	2.79	1.94	1.94	4.17	3.74	2.79	1.94	1.94	4.17	3.74	2.79	1.95	1.95	4.17	3.74	2.79	1.95	1.95	4.17	3.74	2.79	1.95
		2	8.16	6.49	3.83	2.14	2.14	8.22	6.64	4.09	2.39	2.39	8.30	6.78	4.32	2.68	2.68	8.30	6.78	4.32	2.68	2.68	8.30	6.78	4.32	2.68	2.68	8.30	6.78	4.32	2.68
		3	11.03	7.77	3.97	1.87	1.87	11.09	7.85	4.08	1.97	1.97	11.22	8.18	4.38	2.22	2.22	11.22	8.18	4.38	2.22	2.22	11.22	8.18	4.38	2.22	2.22	11.22	8.18	4.38	2.22
	3	1	4.16	3.74	2.79	1.93	1.93	4.17	3.72	2.78	1.94	1.94	4.16	3.74	2.76	1.94	1.94	4.16	3.74	2.76	1.94	1.94	4.16	3.74	2.76	1.94	1.94	4.16	3.74	2.76	1.94
		2	8.15	6.47	3.84	2.13	2.13	8.25	6.66	4.09	2.39	2.39	8.34	6.79	4.34	2.65	2.65	8.34	6.79	4.34	2.65	2.65	8.34	6.79	4.34	2.65	2.65	8.34	6.79	4.34	2.65
		3	11.06	7.78	3.96	1.86	1.86	11.06	7.86	4.07	1.94	1.94	11.36	8.13	4.34	2.28	2.28	11.36	8.13	4.34	2.28	2.28	11.36	8.13	4.34	2.28	2.28	11.36	8.13	4.34	2.28
0.61	1	1	4.16	3.75	2.78	1.94	1.94	4.15	3.75	2.80	1.95	1.95	4.18	3.73	2.78	1.91	1.91	4.18	3.73	2.78	1.91	1.91	4.18	3.73	2.78	1.91	1.91	4.18	3.73	2.78	1.91
		2	8.12	6.48	3.85	2.13	2.13	8.23	6.63	4.11	2.45	2.45	8.31	6.80	4.28	2.74	2.74	8.31	6.80	4.28	2.74	2.74	8.31	6.80	4.28	2.74	2.74	8.31	6.80	4.28	2.74
		3	10.94	7.75	3.96	1.86	1.86	11.05	7.80	4.11	1.99	1.99	11.30	8.15	4.38	2.33	2.33	11.30	8.15	4.38	2.33	2.33	11.30	8.15	4.38	2.33	2.33	11.30	8.15	4.38	2.33
	2	1	4.17	3.75	2.79	1.95	1.95	4.18	3.75	2.78	1.93	1.93	4.17	3.75	2.82	1.96	1.96	4.17	3.75	2.82	1.96	1.96	4.17	3.75	2.82	1.96	1.96	4.17	3.75	2.82	1.96
		2	8.15	6.45	3.87	2.14	2.14	8.24	6.66	4.12	2.42	2.42	8.28	6.75	4.34	2.61	2.61	8.28	6.75	4.34	2.61	2.61	8.28	6.75	4.34	2.61	2.61	8.28	6.75	4.34	2.61
		3	11.03	7.73	3.96	1.84	1.84	11.14	7.80	4.06	1.97	1.97	11.37	8.08	4.27	2.23	2.23	11.37	8.08	4.27	2.23	2.23	11.37	8.08	4.27	2.23	2.23	11.37	8.08	4.27	2.23
	3	1	4.16	3.73	2.79	1.95	1.95	4.17	3.74	2.78	1.95	1.95	4.17	3.74	2.79	1.94	1.94	4.17	3.74	2.79	1.94	1.94	4.17	3.74	2.79	1.94	1.94	4.17	3.74	2.79	1.94
		2	8.15	6.45	3.83	2.14	2.14	8.22	6.64	4.09	2.42	2.42	8.30	6.78	4.30	2.65	2.65	8.30	6.78	4.30	2.65	2.65	8.30	6.78	4.30	2.65	2.65	8.30	6.78	4.30	2.65
		3	11.01	7.75	3.95	1.83	1.83	11.04	7.86	4.02	1.99	1.99	11.18	8.19	4.39	2.30	2.30	11.18	8.19	4.39	2.30	2.30	11.18	8.19	4.39	2.30	2.30	11.18	8.19	4.39	2.30

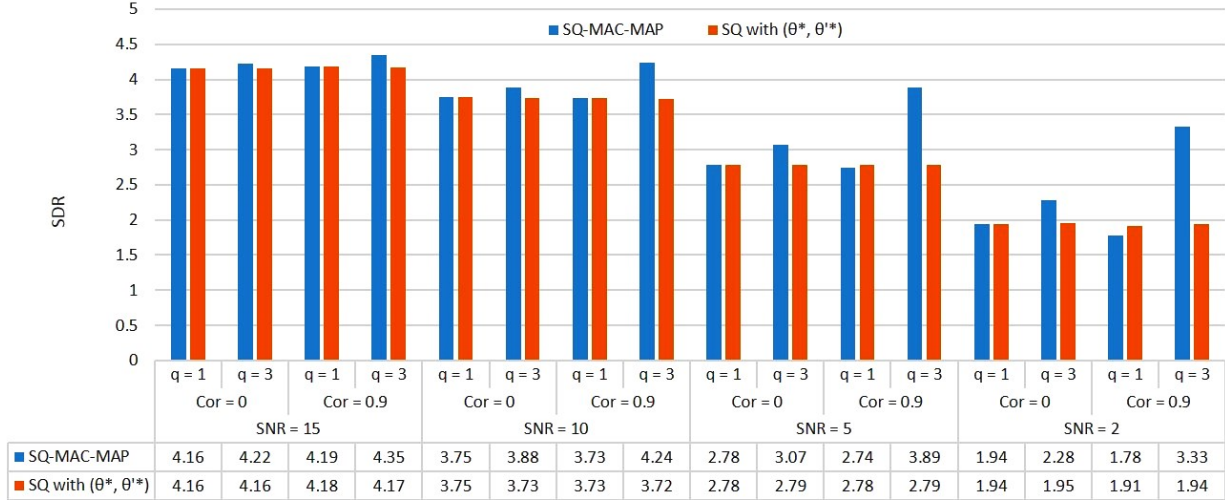


Fig. 6: Simulation SDR results (in dB) of joint MAP decoding and instantaneous joint decoding (θ^* , θ'^*) for two binary-quantized correlated Gaussian sources with Markovian correlation parameter. The channel model is a MAC with two orthogonal NBNDQ-QB, with $M = \alpha = 1$ and identical parameters (Cor , SNR, q); $q = 1, 3$ and $Cor = 0, 0.9$. Source parameters are $\phi_{av} = 0.61$, $\phi_0 = -0.31$, $\phi_1 = 0.81$ and $(t_{\phi_0\phi_0}, t_{\phi_1\phi_1}) = (0.1, 0.8)$. SQs with $n = 1$ are used.

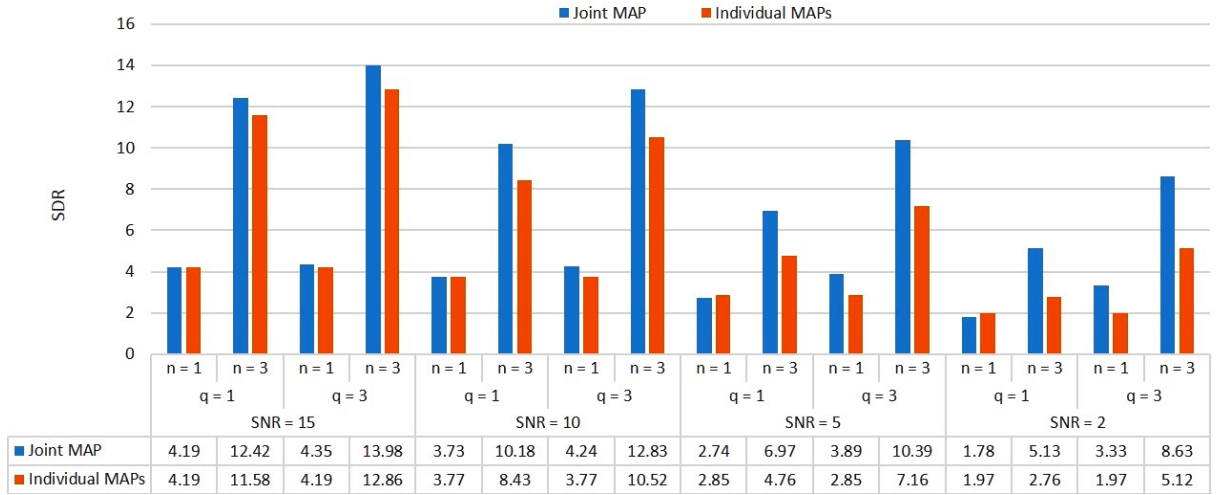


Fig. 7: Simulation SDR results (in dB) of joint MAP decoding and having two independently designed MAP decoders for two binary-quantized correlated Gaussian sources with Markovian correlation parameter. The channel model is a MAC with two orthogonal NBNDQ-QB, with $M = \alpha = 1$, $Cor = Cor' = 0.9$ and identical parameters (SNR, q); $q = 1, 3$. Source parameters are $\phi_{av} = 0.61$, $\phi_0 = -0.31$, $\phi_1 = 0.81$ and $(t_{\phi_0\phi_0}, t_{\phi_1\phi_1}) = (0.1, 0.8)$. SQs with $n = 1, 3$ are used.